

POST – ADDITIVE PROCESSING AND MANUFACTURING OF UAV AIRFRAMES

By

© 2016

Dhruv Chawla

M.S., University of Kansas, 2016

B.E., Manipal Institute of Technology, 2014

Submitted to the graduate degree program in Aerospace Engineering and the Graduate Faculty of the University of Kansas in partial fulfillment of the requirements for the degree of Master of Science.

Graduate Director: Dr. Zhongquan Zheng

Chair: Dr. Ronald Barrett

Committee Member 1: Dr. Haiyang Chao

Committee Member 2: Dr. Huixuan Wu

Honorary Committee Member: Dr. Richard Bramlette

Date Defended: 14 December 2016

The thesis committee for Dhruv Chawla certifies that this is the approved version
of the following thesis:

**POST – ADDITIVE PROCESSING AND MANUFACTURING OF
UAV AIRFRAMES**

Graduate Director: Dr. Zhongquan Zheng

Chair: Dr. Ronald Barrett

Committee Member 1: Dr. Haiyang Chao

Committee Member 2: Dr. Huixuan Wu

Honorary Committee Member: Dr. Richard Bramlette

Date Defended: 14 December 2016

Abstract

Improving manufacturing techniques to minimize costs have always been the ultimate goal for engineers since the dawn of technology. Working toward making the end product as affordable as possible without compromising on its quality is not just a skill set to develop but also, art. This thesis deals with changing the approach to the manufacturing of the patented XQ-139 UAV by using alternative materials to reduce production costs and time. Retaining the overall structure and utility of the UAV while eliminating the high costs to produce is the primary goal. It also includes tests performed on the new UAV airframe to prove this hypothesis and compare it to the results of the original airframe. The objective is to prove that the new airframe can cope with the structural and performance demands of the original XQ-139A, while reducing the total costs to manufacture it. This thesis only deals with the processing and manufacturing of the new XQ-139A airframe. No flight tests are involved.

Acknowledgements

The author would first like to thank his academic and thesis advisor, Dr. Ron Barrett for his continuous motivation, not just during his thesis work but from the first day of Graduate school.

The author will be indebted to him for all the knowledge and experience gained under his tutelage.

Secondly, the author would like to thank Dr. Richard Bramlette for his continuous support and guidance through the entire thesis project.

Lastly, the author expresses his profound gratitude to Dr. Haiyang Chao and Dr. Huixuan Wu for graciously accepting to sit on his committee and providing their immense knowledge and experience.

Table of Contents

- 1 Introduction and Background1
 - 1.1 History.....3
 - 1.1.1 Quadcopter3
 - 1.1.2 Convertible Aircrafts.....4
 - 1.1.3 XQ-139.....5
 - 1.2 Objective5
- 2 Vacuum Forming7
 - 2.1 Introduction7
 - 2.2 History & Working7
 - 2.3 Application8
 - 2.4 Alternative Methods.....9
 - 2.4.1 Injection Molding9
 - 2.4.2 Rotational Molding.....10
 - 2.5 Setup.....11
 - 2.6 Conclusion and Recommendation12
 - 2.6.1 Conclusion.....12
 - 2.6.2 Recommendations.....12
- 3 Mold Manufacturing13
 - 3.1 Introduction13
 - 3.2 Fabrication Process13
 - 3.2.1 Additive Processing – 3D Printing13
 - 3.2.2 Reverse Mold Processing15
 - 3.2.3 Mold Processing17
 - 3.3 Mold Components.....18
 - 3.3.1 Half Quadrants.....19
 - 3.3.2 Wing Caps20
 - 3.4 Conclusion and Recommendations.....24
 - 3.4.1 Conclusion.....24
 - 3.4.2 Recommendations.....24

| | | |
|-------|--------------------------------------|-----|
| 4 | Design Iterations | 25 |
| 4.1 | Introduction | 25 |
| 4.2 | Tools and Equipment | 25 |
| 4.2.1 | Hot-Wire Cutter | 25 |
| 4.2.2 | Other equipment | 28 |
| 4.3 | Iterations | 29 |
| 4.3.1 | Iteration #1 | 29 |
| 4.3.2 | Iteration #2 | 35 |
| 4.3.3 | Iteration #3 | 37 |
| 4.3.4 | Iteration #4 | 44 |
| 4.4 | Conclusion and Recommendations | 51 |
| 4.4.1 | Conclusion | 51 |
| 4.4.2 | Recommendations | 51 |
| 5 | Cost comparison | 52 |
| 5.1 | Introduction | 52 |
| 5.2 | Material Costs | 52 |
| 5.3 | Labor Costs | 53 |
| 5.4 | Total Costs | 54 |
| 5.5 | Conclusion and Recommendations | 55 |
| 5.5.1 | Conclusion | 55 |
| 5.5.2 | Recommendations | 55 |
| 6 | Load Testing | 56 |
| 6.1 | Introduction | 56 |
| 6.2 | Load Test | 56 |
| 6.2.1 | Objective | 56 |
| 6.2.2 | Planning and Groundwork | 57 |
| 6.2.3 | Setup | 71 |
| 6.2.4 | Results | 79 |
| 6.3 | Conclusion and Recommendations | 105 |
| 6.3.1 | Conclusion | 105 |
| 6.3.2 | Recommendations | 105 |

| | | |
|-----|--|-----|
| 7 | Conclusion and Recommendations..... | 106 |
| 7.1 | Conclusion..... | 106 |
| 7.2 | Recommendations..... | 107 |
| 8 | Future Work..... | 109 |
| 9 | References | 110 |
| | Appendix A: Process of Manufacturing the Polycarbonate XQ-139A | |

List of Figures

| | |
|--|----|
| Figure 1.1 DJI Phantom 1 (Recreational Drone) [1]..... | 1 |
| Figure 1.2 Predator launching a Hell-Fire Missile [3] | 2 |
| Figure 1.3 MQ – 9 Reaper [4] | 2 |
| Figure 1.4 Oehmichen No 2 Quadcopter [6] | 3 |
| Figure 1.5 Convair XFY-1 “Pogo” [12]..... | 4 |
| Figure 2.1 Vacuum Forming process [14]..... | 8 |
| Figure 2.2 Injection Molding process [16] | 9 |
| Figure 2.3 Rotational Molding process [18]..... | 10 |
| Figure 2.4 Vacuum former setup | 11 |
| Figure 3.1 MakerBot Z18 Replicator [20]..... | 14 |
| Figure 3.2 Refined 3D printed parts of sections of the upper and lower wing leading edges..... | 15 |
| Figure 3.3 3D Printed part before reverse molding in empty container..... | 16 |
| Figure 3.4 Cured Silicone reverse-mold after being taken out of container | 16 |
| Figure 3.5 Refined mold sample made from black plastic resin | 18 |
| Figure 3.6 2 Octant molds placed back-to-back | 19 |
| Figure 3.7 4-Piece Octant molds placed on vacuum former platform | 20 |
| Figure 3.8 Sections of the leading edge that would be made into molds..... | 21 |
| Figure 3.9 Fabricated wing cap sections using black plastic resin | 21 |
| Figure 3.10 4 Sets of fabricated wing caps..... | 22 |
| Figure 3.11 4 Sets of wing caps placed back-to-back on the vacuum former platform..... | 23 |
| Figure 4.1 Conventional Hot-Wire Cutter [24] | 26 |
| Figure 4.2 Hot-Wire Cutter developed by author | 27 |
| Figure 4.3 T-Slot beams used | 27 |
| Figure 4.4 Wire of the Hot-Wire Cutter when it is red hot | 28 |
| Figure 4.5 Vacuum formed airframe octants..... | 30 |
| Figure 4.6 Result after complete run through the Hot Wire Cutter | 31 |
| Figure 4.7 Octant sections of the airframe | 32 |
| Figure 4.8 Quadrant airframe guide tool..... | 33 |
| Figure 4.9 Airframe quadrant after gluing 2 octants..... | 34 |

| | |
|--|----|
| Figure 4.10 Quadrant joints showing many complex curves to be glued | 35 |
| Figure 4.11 Modified octant molds with new pods | 36 |
| Figure 4.12 Lower wing leading edge section CAD..... | 37 |
| Figure 4.13 Upper wing leading edge section CAD | 38 |
| Figure 4.14 Formed polycarbonate wing caps over the molds | 39 |
| Figure 4.15 Taper of fuselage section making it hard to pull the molds out of the formed Polycarbonate | 40 |
| Figure 4.16 Cuts made along pod section to make it easier to pull lower wing cap mold out | 41 |
| Figure 4.17 Cuts made over fuselage section to make it easier to pull lower wing cap mold out | 41 |
| Figure 4.18 Formed polycarbonate wing caps after pulling out molds..... | 42 |
| Figure 4.19 ‘Cleaned – up’ wing caps after flashing had been cut off | 42 |
| Figure 4.20 Upper wing cap not fitting over leading edge properly..... | 43 |
| Figure 4.21 Leading edge of upper wing after being cut off..... | 44 |
| Figure 4.22 Upper wing cap after being glued to the wing | 45 |
| Figure 4.23 Lower wing cap after being fitted and glued into place | 46 |
| Figure 4.24 No overlap between the 2 fuselage sections of the quadrants | 47 |
| Figure 4.25 Polycarbonate strip added to close the gap..... | 48 |
| Figure 4.26 Half airframe of the XQ-139A..... | 49 |
| Figure 4.27 Complete polycarbonate airframe of the XQ-139A..... | 50 |
| Figure 6.1 Carbon tube used for the spar of the wings | 58 |
| Figure 6.2 Spar being held in place after applying epoxy resin in the lower wing with a clamp and a clip | 59 |
| Figure 6.3 4 sets of half airframes without spars present in the wings | 60 |
| Figure 6.4 4 sets of half airframes with spars present in the wings | 61 |
| Figure 6.5 Motor used for the XQ-139A..... | 62 |
| Figure 6.6 Half airframe after the pod getting cut | 63 |
| Figure 6.7 Design of motor mount..... | 64 |
| Figure 6.8 The 2 carbon tubes used to make the motor mount mold..... | 65 |
| Figure 6.9 The 2 carbon tubes kept in this arrangement to make the mold | 65 |
| Figure 6.10 Cured motor mount molds | 66 |
| Figure 6.11 ‘Cleaned – up’ polycarbonate motor mount | 67 |
| Figure 6.12 Motor secured and glued into the mount | 68 |

| | |
|--|----|
| Figure 6.13 Motor mount being secured and glued to the inside of the pod..... | 68 |
| Figure 6.14 Smoothing leading edge of lower wing using a sanding drum | 69 |
| Figure 6.15 Half Graphite – Epoxy airframe..... | 70 |
| Figure 6.16 Wing spar integrated into the lower wing..... | 70 |
| Figure 6.17 Half airframe sitting on the 2 octant molds for support | 72 |
| Figure 6.18 MDF (Medium Density Fiberboard) being fastened by the table vice..... | 73 |
| Figure 6.19 Half airframe and octant molds fastened to the MDF | 74 |
| Figure 6.20 Pre-calibrated weights used for load testing | 75 |
| Figure 6.21 Load carrying cap..... | 76 |
| Figure 6.22 Thread tied around load carrying cap..... | 76 |
| Figure 6.23 Thin carbon rod taped to wing tip | 77 |
| Figure 6.24 Scale clamped to vice on the floor | 78 |
| Figure 6.25 Top View of XQ-139 A CAD showing 12 mm clearance between propellers (Scale 1:4) | 79 |
| Figure 6.26 Buckling at the trailing edge of the lower wing of the monocoque 10 mil thick airframe wing..... | 80 |
| Figure 6.27 Extreme buckling near the lower wing root of the monocoque 10 mil thick airframe | 81 |
| Figure 6.28 Buckling at the trailing edge of the lower wing of the monocoque 15 mil thick airframe wing..... | 82 |
| Figure 6.29 Extreme buckling near the lower wing root of the monocoque 15 mil thick airframe | 83 |
| Figure 6.30 Buckling at the trailing edge of the lower wing of the monocoque 20 mil thick airframe wing..... | 84 |
| Figure 6.31 Extreme buckling near the lower wing root of the monocoque 20 mil thick airframe | 85 |
| Figure 6.32 5 lbs dumbbell hung using a steel wire | 86 |
| Figure 6.33 Buckling at the trailing edge of the lower wing of the monocoque 30 mil thick airframe wing..... | 87 |
| Figure 6.34 Failure of the load carrying cap undergoing a load of 2463 lbs-f..... | 88 |
| Figure 6.35 Failed load carrying cap..... | 88 |
| Figure 6.36 Failure occurring at the lower wing cap of the 10 mil thick half airframe with spars | 89 |
| Figure 6.37 Almost no buckling along the trailing edge of the lower wing of the 10 mil thick half airframe with spars..... | 90 |

| | |
|---|-----|
| Figure 6.38 Significant buckling causing failure at the trailing edge of the lower of the 15 mil thick half airframe with spars | 91 |
| Figure 6.39 Extreme buckling at trailing edge of the 15 mil thick half airframe with spars causing it to open up | 92 |
| Figure 6.40 Failure at the trailing edge of the lower wing of the 20 mil thick half airframe with spars..... | 93 |
| Figure 6.41 Failure occurring due to the fuselage section overlap opening up in the 30 mil thick half airframe with spars | 94 |
| Figure 6.42 Slight deflection of the Graphite – Epoxy airframe at | 95 |
| Figure 6.43 High deflection of the Graphite – Epoxy wing without spars | 96 |
| Figure 6.44 Comparison of deflection plots of all types of XQ-139A airframes | 98 |
| Figure 6.45 Magnified comparison of deflection plots of all types of XQ-139A airframes | 102 |
| Figure 6.46 Comparing load test results with benchmark tests | 104 |

List of Tables

| | |
|---|-----|
| Table 5.1 Material cost comparison [27]..... | 52 |
| Table 5.2 Labor cost comparison [27] | 54 |
| Table 5.3 Total cost comparison..... | 54 |
| Table 6.1 Comparison of wing deflections at various loads between different types of airframes | 97 |
| Table 6.2 Total Weight comparison of different types of XQ-139A airframes | 100 |
| Table 6.3 Airframes undergoing propeller contact at extreme flight loads..... | 101 |

List of Acronyms

| Acronym | Description |
|----------------|--------------------------------------|
| 3D |Three Dimensional |
| ABS |Acrylonitrile Butadiene Styrene |
| CAD |Computer Aided Design |
| MDF |Medium Density Fiberboard |
| PC |Polycarbonate |
| PE |Polyethylene |
| PETG |Polyester Copolymer |
| PMMA |Acrylic |
| PP |Polypropylene |
| PS |Polystyrene |
| PVC |Polyvinyl Chloride |
| RPM |Rotations Per Minute |
| UAV |Unmanned Aerial Vehicles |
| VTOL |Vertical Takeoff and Landing |

1 Introduction and Background

Since the dawn of the 21st century remote controlled flying has become an ever so increasing phenomenon. Because of great advancements in the field of electronics in recent years, it has become possible to scale down these remote-controlled aircrafts, while keeping the costs relatively low and have been introduced to the public for recreational purposes. Everybody would like to own a drone these days that have different kinds of purposes like photography, racing or even general flying.



Figure 1.1 DJI Phantom 1 (Recreational Drone) [1]

The military also has an immense utility for drones ranging from a dime sized quadcopters for surveillance to a turbocharged piston engine powered UAV that carries Hellfire Anti-Tank missiles for all out aerial attacks. [2]



Figure 1.2 Predator launching a Hell-Fire Missile [3]

Although they are so wide spread, manufacturing costs are still high that drive the unit costs for some UAV's up to US \$60 Million. [4]



Figure 1.3 MQ – 9 Reaper [4]

Which is why alternative materials need to be used to improve manufacturing techniques of UAV's to make them more affordable and practical. Changing the types of materials used could seriously affect the unit costs of the final product.

1.1 History

1.1.1 Quadcopter

Quadcopters are a kind of VTOL (Vertical Takeoff and Landing) aircrafts. The word “quad” refers to it having 4 propellers and is often called a ‘Quadrotor Helicopter’. They are different from helicopters not just because of the number of propellers they have but also because all the motors work in unison to vary the pitch, roll, yaw and altitude of the aircraft. Many manned quadcopters were developed in the early 20th century but possessed problems with stability and high pilot work load. [5]

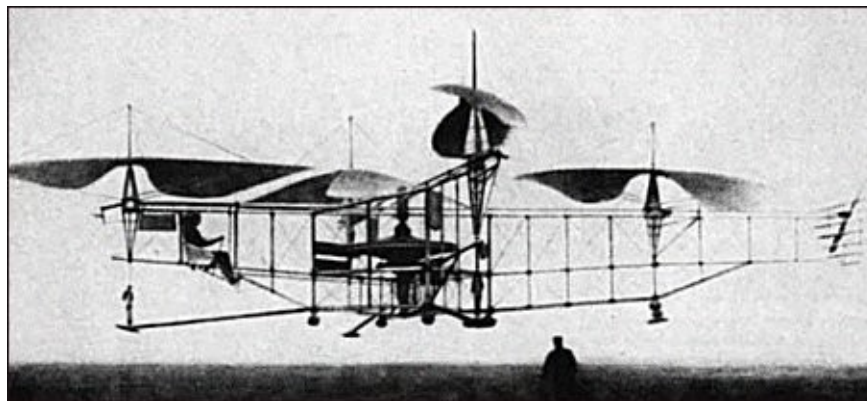


Figure 1.4 Oehmichen No 2 Quadcopter [6]

Quadcopters these days are mostly manufactured in small scales and are controlled remotely. Being small, they are more structurally robust and less expensive than helicopters. [7]

1.1.2 Convertible Aircrafts

Aircrafts possessing the capability of ascending and descending vertically and fly horizontally are known as convertible aircrafts. In other words, they are a combination of helicopters / quadcopters and conventional airplanes. There are several advantages they possess over either of them. The main one being, having the ability to land almost anywhere like a helicopter fly up to speeds north of 300 knots.

The most common type of convertible aircrafts are tilt rotors. A few examples are the V-22 Osprey [8], Bell X-22 [9], AgustaWestland AW609 [10] and the Curtiss-Wright X-19 [11].

Another type of convertible aircraft are the Tailsitters. The name is derived from the way these aircrafts takeoff, by ‘sitting’ on their tails and facing up vertically.



Figure 1.5 Convair XFY-1 “Pogo” [12]

1.1.3 XQ-139

The XQ-139 [12] aircraft is patented and just like any quadcopter it flies remotely with the help of 4 rotors. But it also is a convertible aircraft where it pitches over almost horizontally for forward flight. Here, it generates lift and can perform conventional maneuvers, like roll and pitch with its X-Wing configuration. Variable thrust is used to yaw the aircraft.

The horizontal flight mode is called the “Missile mode” where it can attain high flight speeds. This aircraft has its entire airframe made from Carbon Fiber and possesses high durability while weighing relatively low. The XQ-139 has several potential applications like, recreational, commercial, military or even industrial. [12]

1.2 Objective

The primary objective of this thesis is to reduce the manufacturing and post-processing costs of the XQ-139A UAV. The author believes that this would be possible by using alternate materials which would bring about a change in the manufacturing techniques as well. Time is the main aspect that drives the cost of production up. The author hopes to develop quicker manufacturing methods, if there is a change in the materials used to build the XQ-139A.

There were several alternatives available to replace Carbon Fiber that could potentially help reduce production time. Thermoplastics were an ideal choice due to their excellent ability to be shaped and transformed by alternating the heat applied to them. The author had to choose the type of thermoplastic that would be suitable for the structural and performance demands of the XQ-139A.

After the author successfully assembles an airframe with the new material, it would have to be tested to prove that it could handle extreme flight conditions without failing in any way. The results

would then be compared to the test results of an existing Carbon – Fiber airframe. Cost to manufacture the new airframe would also have to be cut down by a reasonable amount to genuinely prove to be more pragmatic than the Carbon Fiber XQ-139A.

2 Vacuum Forming

2.1 Introduction

This chapter consists of the background and working of Vacuum forming. It covers the functionality and application of the Vacuum Former and mentions a few alternate methods of molding. In this chapter, the author also discusses the setup of the Vacuum Former used for all polycarbonate forming in this report.

2.2 History & Working

Vacuum forming is a process which involves pressing down a heated sheet of plastic over a pre-designed mold, to attain its shape under vacuum. The shape of the mold depends on the desired product. The reason the plastic changes shape upon heating is because it reaches its Glass Transition temperature where its physical properties change such that it becomes soft and rubbery. To ensure proper forming of the plastic against the mold, it is pulled down under vacuum pressure and held there until it regains its original physical properties upon cooling.

Nearly all kinds of thermoplastics can be vacuum formed and are available as sheets of various sizes. The more commonly used materials are listed below. [13]

- Acrylonitrile Butadiene Styrene, ABS
- Polyester Copolymer, PETG
- Polystyrene, PS
- Polycarbonate, PC
- Polypropylene, PP
- Polyethylene (sheet and foamed sheet), PE

- Polyvinyl Chloride, PVC
- Acrylic, PMMA

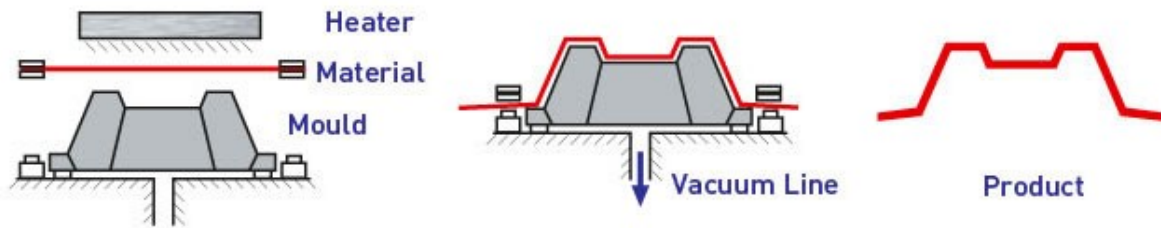


Figure 2.1 Vacuum Forming process [14]

The molds used for forming are generally made from Aluminum, wood or composites. Composite molds are faster and cheaper to produce as compared to aluminum or wood and are usually fabricated through curing liquid resin to a hard solid into any desired shape.

2.3 Application

The author has used Polycarbonate throughout the project to be vacuum formed. Polycarbonates are a group of thermoplastic polymers containing carbonate groups in their chemical structures. [15]

Polycarbonates are used in a wide variety of industries ranging from electronics and data storage to construction and aerospace. They have different grades depending on its application. Polycarbonates can be thermoformed and molded quite easily.

2.4 Alternative Methods

2.4.1 Injection Molding

This form of molding involves ‘injecting’ the desired materials to be molded, into what is known as the ‘mold cavity’. Once all the material is forced into it, it is left to cool and solidifies into the shape of the cavity which is pre-configured, depending on its application. The advantage of Injection Molding is that it can be used to mold a variety of materials ranging from glass and thermoplastics, to metals.

When it comes down to costs, thermoforming, or in this case, vacuum forming is significantly more cost effective. This is mainly because the cost of fabricating the mold cavities for injection molding are very high. Despite low costs, vacuum forming yields good quality products that offers the customer high level of satisfaction.

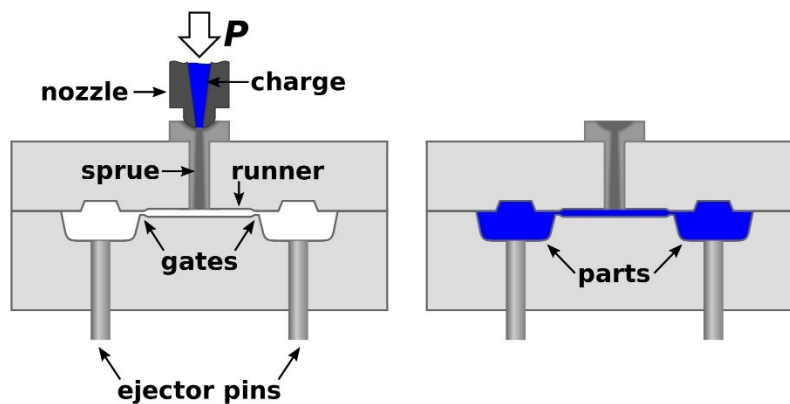


Figure 2.2 Injection Molding process [16]

2.4.2 Rotational Molding

Rotational Molding involves a process in which the material to be molded is added to an enclosed chamber that is made to rotate at a very low RPM (Rotations Per Minute). It undergoes a stage of heating which causes the material to easily flow around the chamber and stick to the walls evenly. Even during the cooling stage the rotation is not stopped until all the material has solidified which avoids any kind of inconsistencies with the final product.

Rotational molding was first developed in the mid-19th century to manufacture metal artillery shells and eventually used to mold plastics by the 1950's. [17]

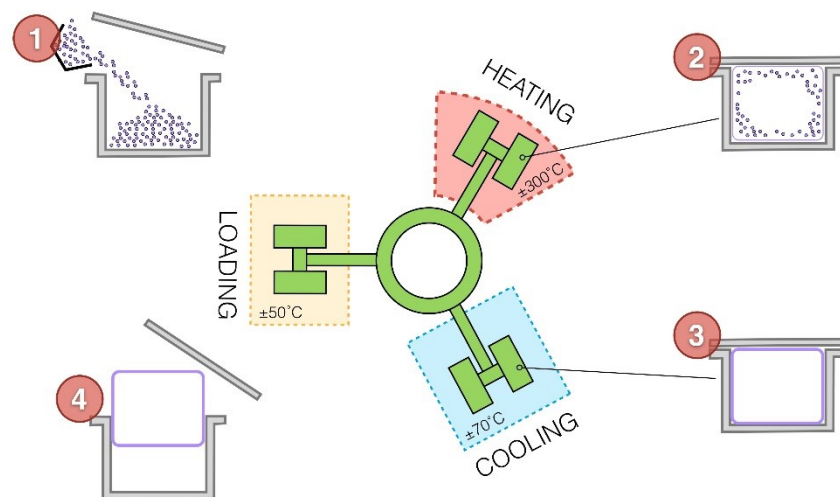


Figure 2.3 Rotational Molding process [18]

The limitations to rotational molding are that the material being molded are sometimes unable to reach certain areas in the mold due to the chamber rotating at the low RPM. This affects the finish and quality of the product. In addition to that, equipment costs are also too high compared to vacuum forming.

2.5 Setup

As mentioned earlier in this chapter that Vacuum Forming is used through the entire project as the primary molding technique.

The setup for the same is shown in figure below.



Figure 2.4 Vacuum former setup

This setup involves a flat rectangular base with dimensions of 17"x12" that consists of evenly spaced holes that are meant to create vacuum. This base is enclosed and is connected to a supersonic wind tunnel. This is done due to the absence of a vacuum pump that the vacuum former

can directly connect to. Since the wind tunnel is connected to one, it acts like a bypass for the vacuum former to generate vacuum on its platform.

Any mold desired to be vacuum formed is placed on this base. Above this base is a heating coil that heats up the Polycarbonate to its Glass Transition Temperature. There is a moving carrier frame between the base and the heating coil that the polycarbonate is fixed to, while performing a vacuum molding process. Once this frame is set up close to the coil the polycarbonate heats up until it starts to sag due to its change in physical property at the glass transition temperature. At that moment, the frame is forced all the way down onto the base for the polycarbonate to take the shape of the mold and the heat is turned off. The Polycarbonate instantly cools and hardens to its original physical property and maintains the shape of the mold.

2.6 Conclusion and Recommendation

2.6.1 Conclusion

The author concludes that;

- Polycarbonate will be used as the material to manufacture the XQ-139A;
- The vacuum forming process has been chosen for all the polycarbonate molding in this report.

2.6.2 Recommendations

The author recommends that;

- A greater number of molding techniques be discussed to confirm that Vacuum Forming is still the most pragmatic molding process to be used in this report.

3 Mold Manufacturing

3.1 Introduction

This chapter involves the different molds that were developed to be Vacuum formed, by the author, and covers the different processes through which they were fabricated.

Since the airframe of the XQ-139A is complicated with several complex curves it cannot be vacuum formed with just a couple of molds. It was broken down to several sections to finally achieve its complete airframe. The author went through several iterations to achieve an efficient manufacturing process that are explained in detail, in Chapter 4.

The following sub-sections of Chapter 3 explain the multiple stages of mold manufacturing employed by the author.

3.2 Fabrication Process

This sub-section will cover the different stages of fabrication that the author went through to finally achieve the desired molds. The sections that follow were the order in which the molds were fabricated.

3.2.1 Additive Processing – 3D Printing

As discussed in Chapter 2 the author found Composite molds to be the cheapest and most efficient compared to other materials. To fabricate composite molds, reverse molds should be made for the liquid resin to be poured into and solidify.

To produce these Reverse Molds, the desired molds were designed and modified by CAD on SolidWorks to be 3D Printed. The MakerBot Z18 Replicator [19] was used for 3D Printing.



Figure 3.1 MakerBot Z18 Replicator [20]

These 3D printed sections had a few inconsistencies with the surface finish on the parts. To rectify that, the author sanded the surface and glazed it with Glazing and Spot Putty [21] to fill in any gaps to achieve a smooth and consistent surface finish.

After applying the putty the section was left to dry for 15 – 20 minutes and the unwanted regions were then sanding off the. The finished product is shown in the figure below.



Figure 3.2 Refined 3D printed parts of sections of the upper and lower wing leading edges

3.2.2 Reverse Mold Processing

Reverse Mold is referred to the mold that is the exact inverse of the desired mold to be vacuum formed. The author chose to use Liquid Silicone [22] to create these reverse molds simply by pouring liquid silicone around the 3D Printed parts mentioned in the previous sub-section.

Before pouring the liquid, it is mixed with a catalyst for shorter curing time. The process involved placing the 3D printed parts in an enclosed container into which the Silicone was poured. The following figures shows the empty container into which the liquid silicone was poured and the final reverse mold after curing.



Figure 3.3 3D Printed part before reverse molding in empty container

The Silicone reverse mold that was obtained at the end of its curing process is shown in the figure below.



Figure 3.4 Cured Silicone reverse-mold after being taken out of container

3.2.3 Mold Processing

The author chose Urethane Resin [23] as the composite material for the fabrication of all the molds.

After the reverse-mold had cured it was ready to be used to form the final mold for the vacuum forming process. This process involved pouring the liquid Plastic Resin into the reverse mold and left to be cured for 30 minutes to 4 hours, depending on the curing speed of the resin used. The slow curing plastic resin has mostly been used by the author to form the molds.

Before pouring, 2 parts of equal volumes are mixed, one being the Plastic resin (Part – A) and the second being the catalyst (Part – B) for fast curing of the mold.

After the Plastic resin has cured, the Mold is removed from the Silicone reverse mold. Like the Post-processing stage, this Mold is filed and sanded to rectify its inconsistencies and glazed with putty, if needed, to eliminate any rough surface. This is required to achieve a smooth and consistent vacuum formed product.

The final refined mold sample is shown in the figure below. This is simply a sample mold to show what the final product would look like. The different mold components fabricated by the author are discussed in detail in the following sub-section.



Figure 3.5 Refined mold sample made from black plastic resin

3.3 Mold Components

This section discusses all the molds that were fabricated to help achieve all the polycarbonate parts to assemble a complete airframe.

To produce the entire polycarbonate airframe, the author fabricated several molds to be vacuum formed. These molds produced different sections of the airframe that were modified and assembled. There were several design iterations that the author went through to end up with these molds. This will be discussed in the following chapter.

3.3.1 Half Quadrants

The first type of mold was an octant, or half a quadrant, of an entire airframe. Two mirror imaged half quadrants were fabricated through the full mold processing method and then replicated to result in a total of 4 sections. These 4 sections were modified a little to allow the author to efficiently place them back-to-back to successfully vacuum form half the airframe in one vacuum pull. Therefore, 2 cycles of vacuum forming the 4-piece mold would result in 8 half quadrants and yield sections for a complete airframe.

The following figures show the half quadrant molds that were initially fabricated and replicated. They also show how the author placed the 4-piece mold onto the vacuum forming platform.



Figure 3.6 2 Octant molds placed back-to-back



Figure 3.7 4-Piece Octant molds placed on vacuum former platform

3.3.2 Wing Caps

The second set of molds the author fabricated were the sections of the leading edge of both the wings. Once again, there were several design iterations that the author went through to end up with these molds which are discussed further in the following chapter.

The figure below shows the sections of the XQ-139A's wings that were made into molds.

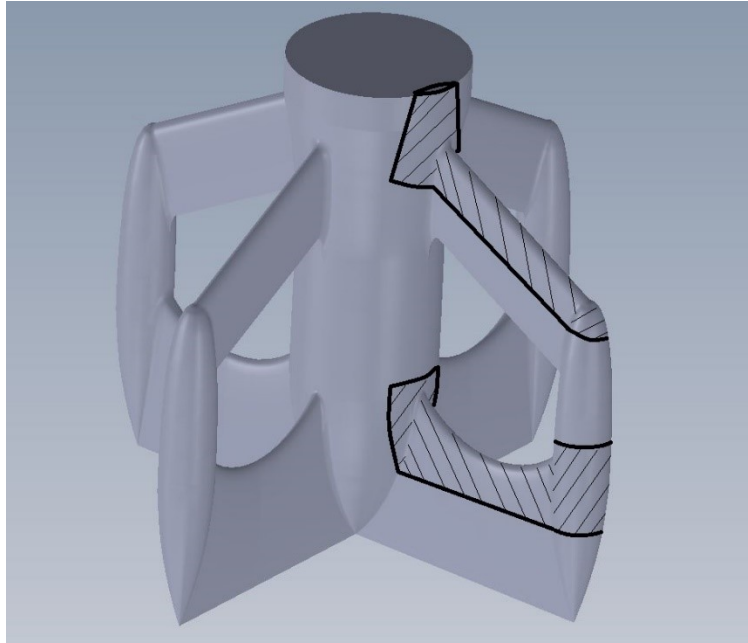


Figure 3.8 Sections of the leading edge that would be made into molds



Figure 3.9 Fabricated wing cap sections using black plastic resin

The author went through the same process as discussed in Section 3.1 to obtain the molds shown above.

Since one airframe of the XQ-139A has 4 sets of wings, it requires 4 wings caps for each of the wings. Therefore, the 2 molds shown above that were fabricated were replicated by the author to obtain a total of 8 mold pieces. 4 caps for the upper wing and 4 for the lower wing. These molds are shown in the figure below.



Figure 3.10 4 Sets of fabricated wing caps

For an efficient vacuum forming cycle, the author placed these molds back-to-back to achieve an entire airframe worth of wing caps for both, the upper and lower wings. The setup of the molds on the vacuum forming platform is shown in the figure below.



Figure 3.11 4 Sets of wing caps placed back-to-back on the vacuum former platform

3.4 Conclusion and Recommendations

3.4.1 Conclusion

The author concludes that;

- The 3 stages of Mold Manufacturing were,
 1. Additive Processing – 3D Printing;
 2. Reverse Mold Processing;
 3. Mold Processing;
- The different Mold Components that were manufactured were,
 1. Half Quadrants (Octants) of the XQ-139A Airframe;
 2. Leading edge wing sections (wing caps) of the upper and lower wings.

3.4.2 Recommendations

The author recommends that;

- Fast curing Plastic Resin be used against the Slow curing version, to save on processing time by up to 88%.

4 Design Iterations

4.1 Introduction

What follows in the sub-sections below are, the tools and equipment used during the manufacturing process and the multiple Iterations the author went through to obtain a complete polycarbonate airframe of the XQ-139A. The primary objective is to minimize time taken, without compromising on quality, to obtain the complete airframe. To do so, every step was optimized or replaced by an alternate method to achieve said objective.

4.2 Tools and Equipment

There were several tools and equipment used throughout this process to achieve the desired result. The main tools that are prominent have been listed below along with their contribution toward the manufacturing process.

4.2.1 Hot-Wire Cutter

The Hot-Wire cutter is a tool used to slice / cut certain materials like foam or most thermoplastics. This tool consists of a thin metal wire under relatively high tension and electrical resistance. The high tension keeps the wire taut to minimize inaccuracies during the cut and the electrical resistance causes it to heat up to temperatures about 200°C. The metal wire is usually made of steel or nichrome. The author has used nichrome wire for the setup.

A common set-up of a Hot-Wire cutter is shown below.



Figure 4.1 Conventional Hot-Wire Cutter [24]

Instead of purchasing an off-the-shelf Hot-Wire Cutter, the author has developed a custom one for this project. It was made by using standard 2"x2" wood blocks, 1"x1" T-slotted Beams [25], a set of L-brackets and a set of screw and washers.

The setup is shown in the figures below.



Figure 4.2 Hot-Wire Cutter developed by author



Figure 4.3 T-Slot beams used

The entire C-shaped beam section as shown in Figure 4.2 Hot-Wire Cutter developed by author is made movable along the vertical beams by loosening the screws on its side and tightening them to fix it into the desired height from the ground. This allows the user to vary the height of the cut.

The figure below shows the wire while it is red hot when 11 V is applied through it.

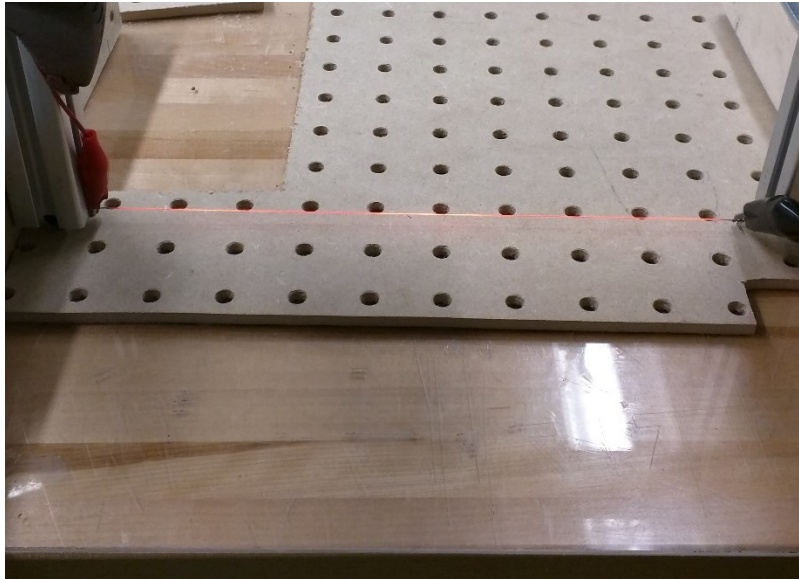


Figure 4.4 Wire of the Hot-Wire Cutter when it is red hot

4.2.2 Other equipment

The author used the Ryobi 1.2 Amp 16 in. Corded Scroll Saw [26] for mostly cutting MDF (Medium Density Fiberboards) sections for different purposes like an even platform for the Hot Wire Cutter to aid in a smooth slide of the material to be cut.

A Drill press was used by the author mainly during the assembly of the Hot Wire cutter.

Another piece of equipment that was used briefly was the Scroll saw with diamond blades that was used in cutting carbon tube, discussed later in the report.

4.3 Iterations

This sub-section involves the various iterations of manufacturing the author went through to finally result in a satisfactory Airframe. It started with an initial idea the author had about preparing certain molds to vacuum form and then bring together. Seeing the results it produced, modifications were made to certain aspects of the procedure to improve the efficiency and outcome of the product. Each time the author made a reasonable alteration to the manufacturing process, it was noted down as a new iteration. These iterations are discussed in detail in the following sections with numerous figures to help the reader understand every characteristic change made by the author.

The author has used polycarbonate sheets of thickness 10 mil (1 mil = 0.001 inches) throughout all the iterations mentions under this sub-section.

4.3.1 Iteration #1

Initially, when the vacuum forming process was relatively new to the author, a few trial runs were performed to find the optimum moment in time to press down the polycarbonate over the mold, after it had reached the glass transition point. After the 4 octant molds were fabricated, the author planned to vacuum form them. Two sheets of polycarbonate would yield in an airframe worth of pieces / octants. The molds were placed back-to-back on the vacuum platform to be used for vacuum forming. After pressing down the polycarbonate under vacuum, it took the shape of the molds. The result is shown in the figure below.



Figure 4.5 Vacuum formed airframe octants

This process was repeated to get two sheets of molded polycarbonate.

The first step from this point was to get rid of the flashing around the formed mold. This was done simply by cutting it off with scissors. Now, there were certain sections that need to be removed to move forward with getting the airframe together.

The author found the Hot Wire Cutter was the quickest and most efficient way to do so. This would involve sliding the whole formed sheet through the hot wire at a certain height from the platform. This height was decided by the author by measuring how much of the polycarbonate needed to be cut. For this process the Voltage for the Hot wire was set to 11V to attain a red-hot wire.

The resultant was a clean cut of the formed sheet. All flashing had been cut off.

The figure below shows what the author obtained after the Hot wire cutting process.



Figure 4.6 Result after complete run through the Hot Wire Cutter

The same process was repeated for the other sheet as well. Now, the remaining section consisted of 4 octants of the airframe, per sheet. The author now had to cut out all eights from both the sheets to have 8 individual octant sections of the XQ-139A. The figure below shows what the octant sections looked like.



Figure 4.7 Octant sections of the airframe

Once these were cut the author formed quadrants by joining 2 octants at an angle of 90 degrees. This is a crucial stage in the making of the airframe because if not done right, the resultant airframe would be deformed. The forming of quadrants was achieved by using a guide tool of a quadrant prepared out of Black plastic resin to obtain a perfect 90-degree section.



Figure 4.8 Quadrant airframe guide tool

This was done by first cutting little flashing off the fuselage section on each octant piece. Then, one of the octants was fastened on half of the guide tool to help improve accuracy while the other was placed by hand onto the other half of the tool. Just before placing the other octant section, glue was applied on the thin fuselage section that would be overlapped by the other half.

The red marking on the tool denoted the center line along which the join had to be made. After joining the 2 sections, slight pressure with the fingers for a few seconds was enough to set the joint. This aided the author to achieve an accurate fuse of 2 eights to form a quadrant of the XQ-139A airframe, that is shown in the figure below.

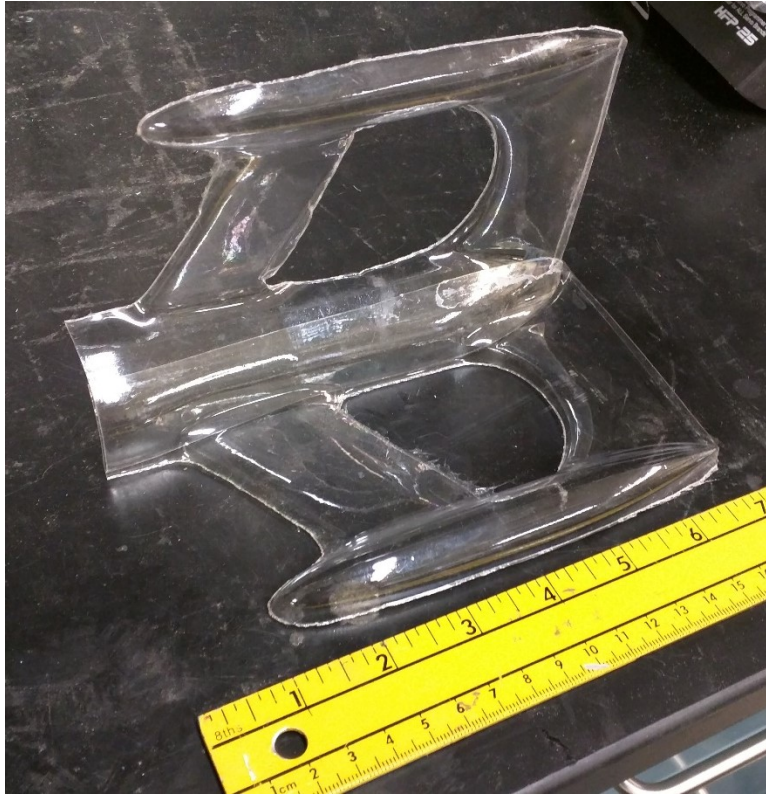


Figure 4.9 Airframe quadrant after gluing 2 octants

This process was repeated to form 4 quadrants.

Now, all the author had to do was join all 4 quadrants to obtain the whole airframe.

The next step involved bringing together 2 quadrants to form a half airframe. This was done by joining the quadrants along the edges of the pods and wings. This involved gluing multiple complex curves together.

A perfect alignment of the 2 quadrants was also a vital aspect to control. It was hard to maintain other edges while attempting to glue down one edge, especially if it was a curved one.

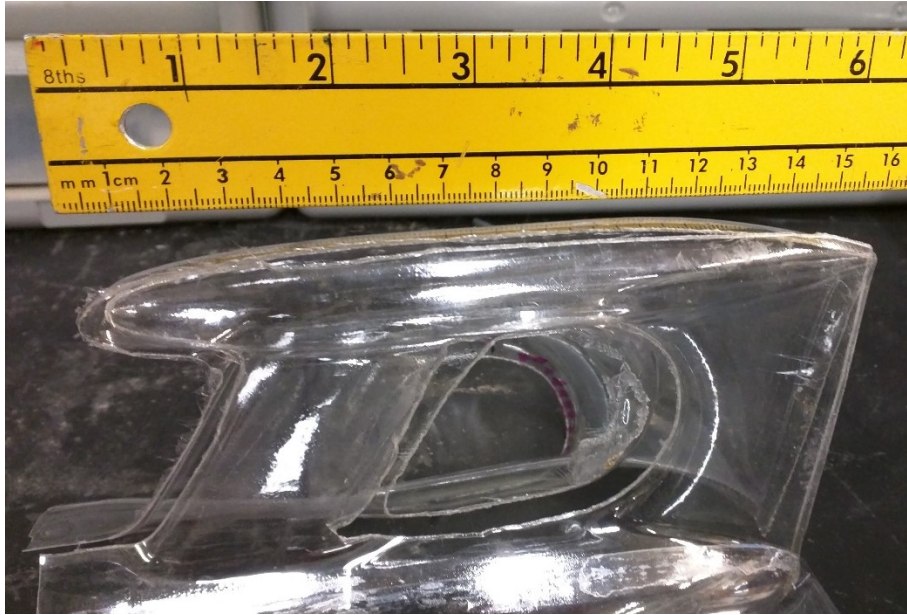


Figure 4.10 Quadrant joints showing many complex curves to be glued

The author found this method of joining the airframe sections together very inefficient and inconsistent. A more reliable process had to be created to achieve a consistent design every time.

The author addressed this problem by changing a few aspects of the process that are explained in the next sub-section.

4.3.2 Iteration #2

The primary issue the author faced in the first iteration of the design process of the XQ-139A was dealing with the complex curves of the pods and leading and trailing edges of the wing. Gluing one curve while maintaining perfect alignment of the other curves was nearly impossible and inconsistent.

The solution to this problem was to eliminate the most complex curve, the nose cone of the pods. The author believed that eliminating that would make it easier to glue the edges together.

Now, to do so, the Resin molds had to be altered. The nose cones of the pods had to be sawed off and filed to achieve a smooth cone tip at the leading edge of the forward wing tip. This is shown in the figure below.



Figure 4.11 Modified octant molds with new pods

Once these molds were modified, the whole vacuum forming process of the 4 octant molds were repeated.

The intermediate stages of hot wire cutting and obtaining sections of octants was also repeated in the same way as explained in the previous sub-section. During the stage where the author joined the 2 quadrants, gluing the pods was simple. It was done by simply applying glue on one of the long edges of the pod to be overlapped and bringing them together. Once this was achieved, the leading and trailing edges of both the wings were yet to be joined.

Due to insufficient room for any overlap, it was very hard to join the leading edges of both the wings. There were problems again with consistency and accuracy with these joints. This stage of the manufacturing process needed to be revisited by the author to develop a better way to obtain a

smooth and consistent leading edge for both wings and at the same time maintain the clean edge joint of the pods.

4.3.3 Iteration #3

The third iteration of the manufacturing process of the XQ-139A involved rectifying the issue of rough inconsistent leading edges of both wings. A method had to be developed to eliminate this issue without affecting the previous solved difficulties. The author came up with an idea to create leading edge ‘caps’ that would go over the leading-edge section of both the wings for it to be smooth and consistent with no chance for error.

So, as shown in section 3.3.2 these wing caps were fabricated by first designing a CAD model on SolidWorks to suit the procedure of 3D printing it. This CAD model is shown in the figure below.

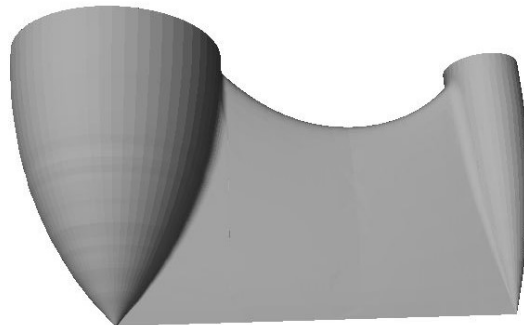


Figure 4.12 Lower wing leading edge section CAD

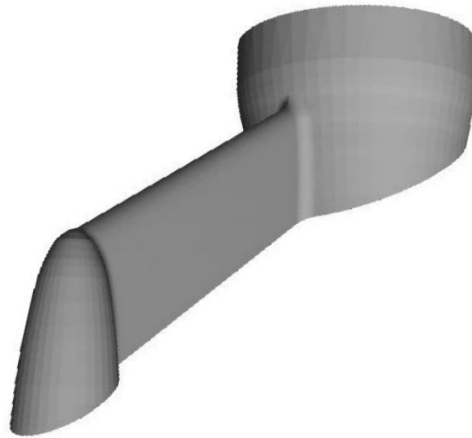


Figure 4.13 Upper wing leading edge section CAD

After getting them 3D printed these sections were fine-tuned by eliminating any anomalies on the surface to obtain an even and smooth product. Now, the molds to be vacuum formed had to be fabricated. These were done by first making a reverse mold out of the 3D printed sections. This process has been explained in section 3.2.2 that is common to all types of molds made in this report. To make the reverse mold, the 3D printed wing caps were placed in an aluminum sheet box, prepared per the cap's size, into which the liquid silicone was poured around the 3D printed caps. After 7-8 hours of curing, the reverse mold is ready. Now, to make the final mold of the wing caps, liquid black plastic resin is poured in the reverse mold and left to cure. Depending on whether it is a slow or fast curing resin, it takes about 30 minutes to a few hours, respectively, to fully cure until it can be removed from the reverse mold for final fine-tuning.

The resultant wing cap molds are now ready to be vacuum formed to form the polycarbonate sections.

The author is always looking for the most efficient ways to vacuum form by wasting the least amount of polycarbonate. Hence, the author decided to form 4 sets of wing caps in one vacuum

pull that would yield sections worth an entire airframe. To do so, 3 additional sets of wing caps should be fabricated. The process of mold fabrication is not as long anymore because there is a set of reverse molds from the initial procedure. Therefore, black plastic resin is poured and cured 3 times to finally obtain a total of 4 sets of wing caps.

For the process of vacuum forming the author places the alike wing caps back-to-back on the platform of the vacuum former. The result of the vacuum formed wing caps is shown in the figure below.



Figure 4.14 Formed polycarbonate wing caps over the molds

To remove the molds from the formed polycarbonate was a challenge the author did not expect, especially for the rear wing's leading edge's mold. This was because of its slightly tapering shape that made it so hard to simply pull it out.

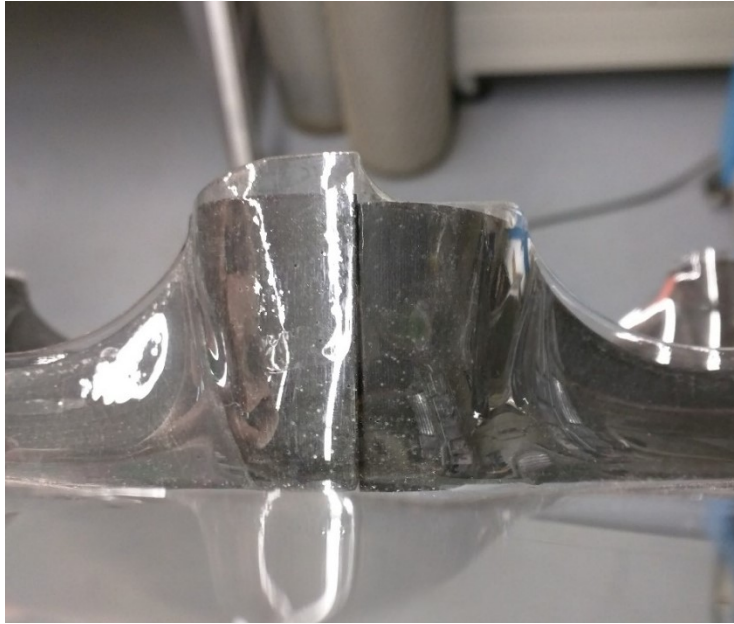


Figure 4.15 Taper of fuselage section making it hard to pull the molds out of the formed Polycarbonate

This problem occurred both, at the pod and the fuselage section of the mold. A couple of cuts were made onto the formed polycarbonate using an 'X-acto blade' to make it easier for the author to push/pull the molds out of the sheet.

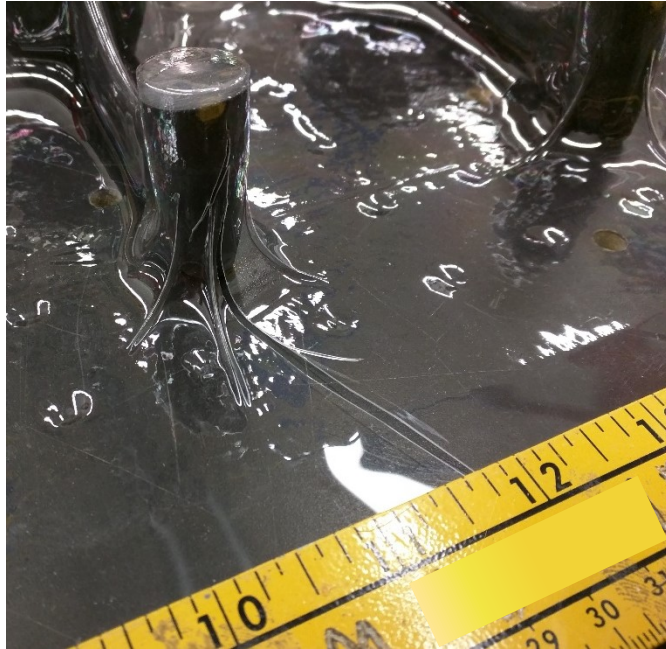


Figure 4.16 Cuts made along pod section to make it easier to pull lower wing cap mold out



Figure 4.17 Cuts made over fuselage section to make it easier to pull lower wing cap mold out

Once this was taken care of, the formed leading edges needed to be cut to be separated from each other.



Figure 4.18 Formed polycarbonate wing caps after pulling out molds

Then all the flashing was cut out from these individual polycarbonate sections. After all the ‘clean-up’ on them, the figure below shows all the sections that were obtained.



Figure 4.19 ‘Cleaned – up’ wing caps after flashing had been cut off

The next procedure was to integrate them into the wings of the XQ-139A and complete the airframe. To do so, first the whole process of creating the quadrants was repeated that is explained in section 4.3.1. The only aspect different is that the modified octant mold is used, where the nose cones of the pods have been eliminated and filed to achieve a smooth converging cone ending at the leading edge of the top wing tip.

Once it was time to bring 2 quadrants together the dilemma the author faced was whether to first glue along the edge of the pod and then glue down the wing caps or vice versa. The former method was finally chosen. Once, this edge was secured it was time to fit in the wing caps, with the upper cap to be glued first. There was a problem the author ran into, in this step. The existing leading edge section of the wing was not allowing the wing cap of the upper wing to fit in all the way down.



Figure 4.20 Upper wing cap not fitting over leading edge properly

This meant that the upper wing chord would increase significantly, by 20% approximately. This was unacceptable to the author and hence had to be revisited to rectify the issue. The next sub-section involves the same and the also covers how it was achieved.

4.3.4 Iteration #4

This sub-section consists of the method by which the author fixed the issue of the wing cap not being able to completely sit all the way to the bottom of the leading edge of the upper wing.

Before gluing together, the 2 quadrants along the pod's edge, the issue was fixed by cutting about half an inch off the leading edge of the upper wing.



Figure 4.21 Leading edge of upper wing after being cut off

This was done so that the wing cap not only sits perfectly now but also has enough overlap to be glued to the wing well. The section that was cut was done by using a pair of regular curved scissors.

The reason those were used is because being curved aided in getting around the complex curves that were present in the wing and pod section of the XQ-139A.

The upper wing cap was then glued to the wing as shown in the figure below.



Figure 4.22 Upper wing cap after being glued to the wing

To glue together the trailing edge of the upper wing, glue was simply applied in the required region on the insides of the same and held in place by using a clip.

The next curve to secure was the leading edge of the lower wing. This was done by fitting the lower wing cap over the section and aligning it just right so that it would sit perfectly over the leading edge. To fix it to the wing, glue was applied to the side flaps of the wing cap and held in place until dry.

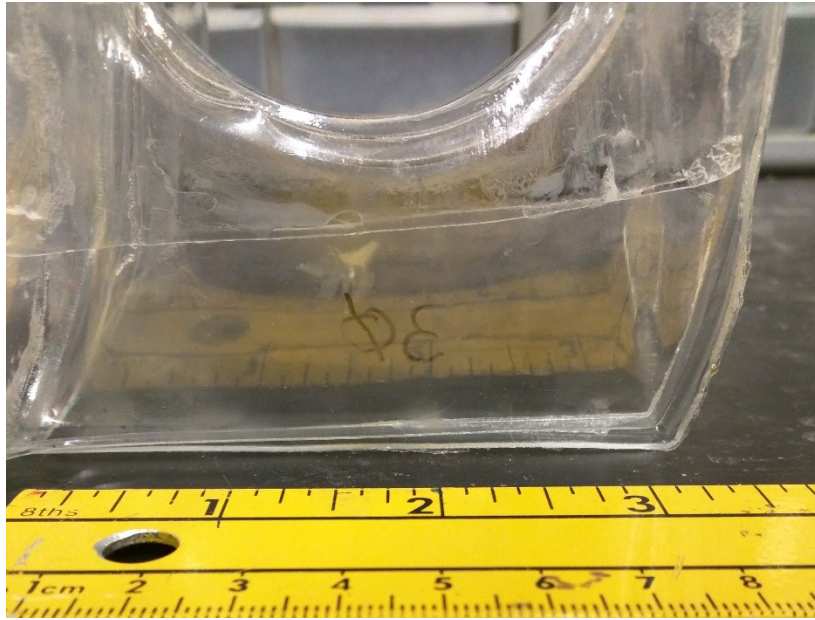


Figure 4.23 Lower wing cap after being fitted and glued into place

The only edge that was still open was the fuselage section between the 2 quadrants.

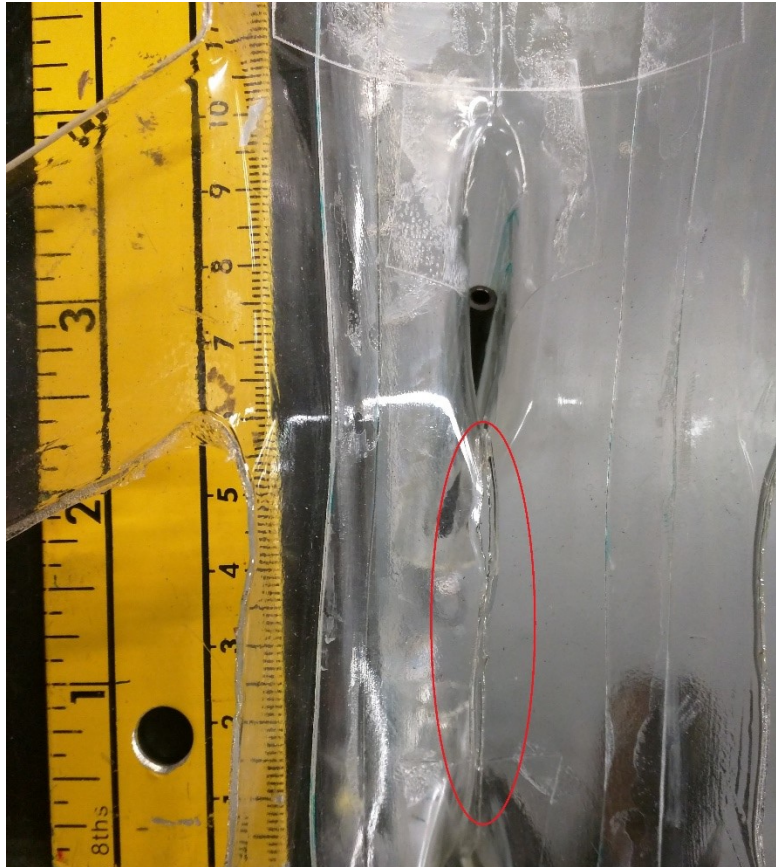


Figure 4.24 No overlap between the 2 fuselage sections of the quadrants

The author noticed that there was no overlap there so came up with a method to glue down a strip of polycarbonate of dimensions 1.5" x 0.5", along the edge, inside the fuselage.



Figure 4.25 Polycarbonate strip added to close the gap

A 20 mil thick sheet of polycarbonate was used for this strip. At the end of this step, half of the airframe of the XQ-139A was obtained.



Figure 4.26 Half airframe of the XQ-139A

This result was satisfactory to the author and stuck to this method to produce the other half of the airframe. Once there were 2 halves ready, the only thing left to do was to get them together and complete the airframe of the XQ-139A. The method remained the same, the difference was that, now 2 sections needed to be glued, on either side of the fuselage. The complete airframe was spray painted black to better observe the outer surface and finish of the airframe.

The completed airframe is shown in the figure below.



Figure 4.27 Complete polycarbonate airframe of the XQ-139A

4.4 Conclusion and Recommendations

4.4.1 Conclusion

The author concludes that,

- A custom Hot-Wire cutter was designed and assembled for all Polycarbonate cutting processes;
- It took 4 manufacturing iterations to obtain the XQ-139A Polycarbonate Airframe.

4.4.2 Recommendations

The author recommends that,

- A bigger Vacuum former platform be used for the 4 sets of wing caps, to allow more room between each set, to achieve a tighter vacuum mold;
- A second airframe should be manufactured to improve its quality and surface finish.

5 Cost comparison

5.1 Introduction

The previous chapter covered the entire procedure the author went through, including all the iterations of manufacturing to achieve the final Polycarbonate airframe. The complete airframe of the XQ-139A was now ready and the author wanted a way to compare it with the original airframe that was fabricated entirely with Carbon Fiber.

This chapter covers the breakdown of the cost for manufacturing the Carbon Fiber, as well as the Polycarbonate XQ-139 Airframe. The author discusses the material and labor costs involved in the entire process and how it affects the total cost.

5.2 Material Costs

The author referred to the cost of the materials used in previous research projects for the XQ-139A UAV, and has compared the two, to better understand it, in the table below.

Table 5.1 Material cost comparison [27]

| Material | Total cost of used material for 1 airframe, US \$ |
|-----------------|--|
| Carbon Fiber | 105 |
| Polycarbonate | 23 |

The primary reason for the difference in cost is because in the carbon fiber airframe materials, like fiber glass and carbon veil have also been used in small amounts that add up to the total material cost. Whereas, nothing but polycarbonate is used in the other airframe.

5.3 Labor Costs

In terms of time taken from scratch to a complete airframe, there is a large difference between the two. Compared to the 7 days it takes to manufacture the Carbon Fiber airframe, the author took less than 4 hours to complete the entire XQ-139A airframe from scratch. This time included vacuum forming the polycarbonate sheets to acquire the required airframe sections, i.e. octants of the airframe and the wing caps, through the whole cutting and gluing process, until the complete airframe was fabricated. It also included the spray painting of the airframe exterior.

For the Carbon Fiber XQ-139A approximately 48 hours are spent that includes quadrants processing and post processing, cutting the pods to add the motors, cleanup of surface and painting. [27]

This meant that the cost to manufacture the XQ-139A reduced by almost an order of magnitude compared to the Carbon Fiber one. This is majorly due to the labor costs involved because manufacturing the Carbon airframe would take 12 times the time it would take for the polycarbonate one.

Labor costs are the major constituent of the total estimated cost to manufacture an airframe of the XQ-139A, whether it is the polycarbonate or the Carbon fiber one. As mentioned above, approximately 48 hours were spent to manufacture the Carbon Fiber XQ-139A, while only 4 hours was spent on the Polycarbonate airframe. The cost of labor was estimated by the author to be \$15 / hour. The table below suggests the total labor costs for each of the airframes.

Table 5.2 Labor cost comparison [27]

| Type of XQ-139A | Total number of hours to manufacture, hours | Cost of labor, US \$ / hour | Total labor costs to manufacture 1 airframe, US \$ |
|------------------------|--|------------------------------------|---|
| Carbon Fiber | 48 | 15 | 720 |
| Polycarbonate | 4 | 15 | 60 |

As seen in the table there is a significant difference between the labor costs of both types of the XQ-139A's. The sole reason for that is the time taken to manufacture the Carbon Fiber airframe that drives its labor costs up.

5.4 Total Costs

The author has not included certain costs for this section like, energy used to operate tools and other machinery, as these are simply hard to estimate and would not cause a big dent in the total costs. Hence, for this report the author is just adding the material and labor costs for each type of airframe to obtain the total manufacturing costs for both. The table below shows the total costs for each airframe.

Table 5.3 Total cost comparison

| Type of XQ-139A | Material costs to manufacture 1 airframe, US \$ | Labor costs to manufacture 1 airframe, US \$ | Total cost to manufacture 1 airframe, US \$ |
|---|--|---|--|
| Carbon Fiber | 105 | 720 | 825 |
| Polycarbonate | 23 | 60 | 83 |
| Percentage drop in Manufacturing Costs for the XQ-139A | | | 89.9% |

As seen in the tables above, there is a significant drop in the manufacturing costs and time with the new material used for the XQ-139A. This proves that using Polycarbonate instead of Carbon Fiber reduced the total costs by almost an order of magnitude.

5.5 Conclusion and Recommendations

5.5.1 Conclusion

The author concludes that,

- The total material costs for the 2 types of XQ-139A Airframes are;
 1. Carbon Fiber: US \$105
 2. Polycarbonate: US \$23
- The total labor costs for the 2 types of XQ-139A Airframes are;
 1. Carbon Fiber: US \$720
 2. Polycarbonate: US \$60
- The total costs for the 2 types of XQ-139A Airframes are;
 3. Carbon Fiber: US \$825
 4. Polycarbonate: US \$83
- The overall percentage drop in manufacturing costs of the XQ-139A is 89.9%.

5.5.2 Recommendations

The author recommends that,

- A detailed cost analysis be performed for the Polycarbonate XQ-139A.

6 Load Testing

6.1 Introduction

The previous chapter proved that the Polycarbonate airframe was significantly cheaper to manufacture. This chapter covers the load testing of the Polycarbonate XQ-139A airframe. It consists of the overall objective of the tests and all the preparation involved in setting it up. The final section deals with the results of the tests, that has been explained with the help of several figures, tables and plots.

To compare the results of the Polycarbonate airframes against the original one, a Half airframe of the original XQ-139A was also tested with and without a wing spar present in its lower wing.

6.2 Load Test

6.2.1 Objective

The author wanted to test the prepared airframe by subjecting it to bending loads and see if the new XQ-139A would be able to handle normal, to extreme flight conditions. To do so, a load testing exercise had to be setup that would mimic the type of loads the airframe would experience during flight.

The primary objective of the load tests of the wings of the XQ-139A was to assess the loads at which failure occurred, if any. The author also wanted to check the load at which the wing would deflect just enough for the propeller to touch one of its neighboring propellers, because even that would be considered a type of failure. To setup a comparison chart for these tests, the author decided to use a variety of polycarbonate airframes of different thicknesses with and without spars through it. Per the results of the tests, the author would select the most suitable thickness for the

polycarbonate based on aspects like, the stiffness and flexural strength of the wings and the gross weight of the airframe (Greater the thickness of the polycarbonate used, greater the weight of the airframe). The results would be displayed in the form of a table with the deflection of the wings of different thicknesses and types, at the given loads and the flexural strength would be represented by plotting the deflection of the wing tip against the load applied to it.

What the author wanted to see was which airframe would not fail at the maximum possible given load during any flight condition, which would be the entire aircraft weight on one wing. The weight on each type of airframe would be different because of the difference in thickness and / or presence of spars, if any.

6.2.2 Planning and Groundwork

Since the XQ-139A had 4 sets of wings, the author figured that testing just one set would be sufficient as they were all identical. It had to be setup in a way that it would be relatively simple to apply controlled loads to the wing undergoing the tests. The said load test and its results are explained in the following sub-sections.

As mentioned in the beginning of this chapter the author wished to test a variety of airframes of different thicknesses, with and without spars present in the wings. Since the entire airframe was not required, the author would set up the test with just half airframes.

6.2.2.1 Airframes

To test the variety of airframes, they had to be fabricated first. So, the author manufactured 2 sets of half airframes of the XQ-139A of thicknesses, 10, 15, 20 and 30 mil. The same method of manufacturing was implemented as discussed in chapter 4. One set of the airframes were going to be tested as they were, a fully monocoque structure. The second set, on the other hand, was going to be integrated with a set of spars through each of its wings to achieve a greater resistance to bending when any load would be applied to it. This was done by using 2.5 inches long Carbon tubes of diameter 0.2 inches, that would fit in perfectly along the span of the wings.



Figure 6.1 Carbon tube used for the spar of the wings

They were cut into the desired lengths by using a Diamond cutting scroll saw. It is like the Scroll Saw discussed in Section 4.2.2, but here, the saw blade had diamonds fixed on its edge for cutting hard or abrasive material.

To integrate the spars to the airframe, these rods were coated with 'Quick Cure 5-minute Epoxy resin' [28] and then were placed at quarter chord of the wings and held in place using clips and / or clamps until they cured. The figures below show the type of epoxy used and how the spars were held in place.



Figure 6.2 Spar being held in place after applying epoxy resin in the lower wing with a clamp and a clip

These were done to the entire second set of half XQ-139A airframes.

At the end of this step, the author had 4 monocoque airframes and 4 airframes with spars, of the XQ-139A.



Figure 6.3 4 sets of half airframes without spars present in the wings



Figure 6.4 4 sets of half airframes with spars present in the wings

6.2.2.2 Motor and Motor Mount

To mimic the actual flight conditions for the load tests as much as possible, the tip pods on each of the airframes were cut out between the two wings to accommodate the motor and the motor mount into it. For the XQ-139A, a Turnigy 1811 Brushless Outrunner 2900kv motor will be used throughout. [29]

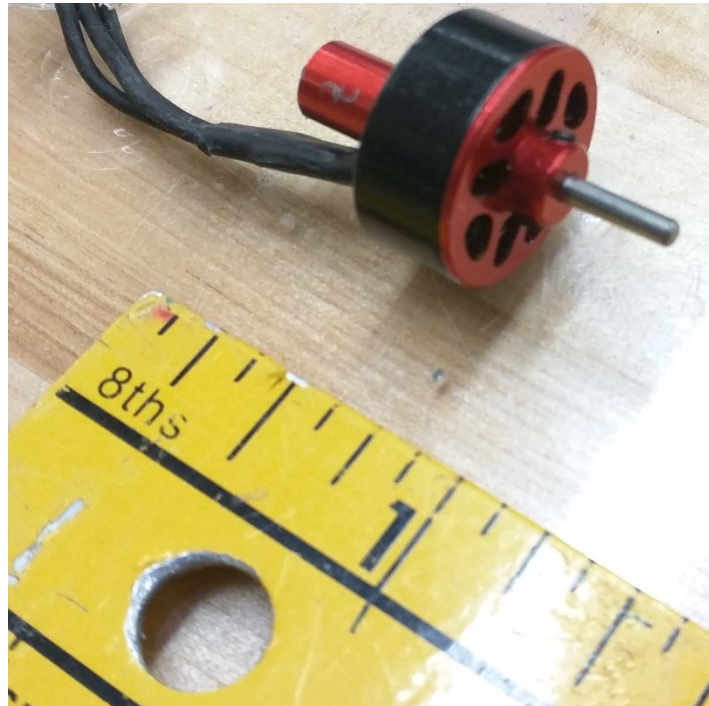


Figure 6.5 Motor used for the XQ-139A

This cut was achieved by using the hot wire cutter by running the airframe through the hot wire, pod first. This was repeated for all 8 half airframes.



Figure 6.6 Half airframe after the pod getting cut

The motor mount had to be such that the motor's shaft onto which the propeller would be fixed faced out of the pod. To do so, the rear casing of the motor needed to be fixed to the motor mount that needed to be secured on the inside of the pod. The author came up with a motor mount design that resembled the figure shown below.

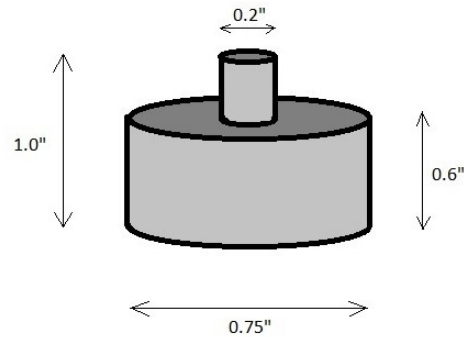


Figure 6.7 Design of motor mount

The author wanted this to be fabricated out of polycarbonate. To do so, a mold had to be prepared to be vacuum formed. The motor mount had to be slightly smaller to the diameter of the inside of the pod to fit in securely. After measuring the pod diameter the author chose the diameter of the mount to be 0.75 inches. To make the mold for the motor mount, a thin carbon tube having an outer diameter of 0.75 inches had been chosen.

The height the author chose the motor mount to be was a total of 1 inch. This part of the mold would be used as the main body of the motor mount. What was now needed was a thin opening to accommodate the motor's rear casing into the mount. To add this feature to the mold, a thin carbon tube of diameter 0.2 inches was chosen that would sit in the center of the 0.75 inch tube as shown in the figures below.



Figure 6.8 The 2 carbon tubes used to make the motor mount mold



Figure 6.9 The 2 carbon tubes kept in this arrangement to make the mold

To make this a solid piece, the author chose to use Epoxy Resin to be filled into it and wait for it to cure. As mentioned earlier, the author liked to be efficient in every step possible, so, 8 sets of motor mount molds were fabricated so that lesser polycarbonate would be wasted when they were vacuum formed and at the same time yield to mounts worth 2 entire airframes. A layer of MDF (Medium Density Fiberboard) was added to the bottom of the mold to give it an added height for the vacuum forming process. This was done so that the fillet the formed polycarbonate would make at the bottom edge of the mold would be extra material to be discarded, without using up any of the useful height needed for the motor mount.



Figure 6.10 Cured motor mount molds

After these mount molds were cured, they were placed on the vacuum former platform as shown in the figure above. The author chose 20 mil thick polycarbonate sheets for the vacuum forming process of the motor mounts.

The figure below shows the formed mounts after being cut from the sheet. The wrinkles formed during the vacuum forming process were also cut out.



Figure 6.11 ‘Cleaned – up’ polycarbonate motor mount

Now, it was time to fix the motor to its mount by securing the rear casing into the mount’s opening.



Figure 6.12 Motor secured and glued into the mount

This Motor – mount setup was then secured inside the airframe pod as shown in the figure below.

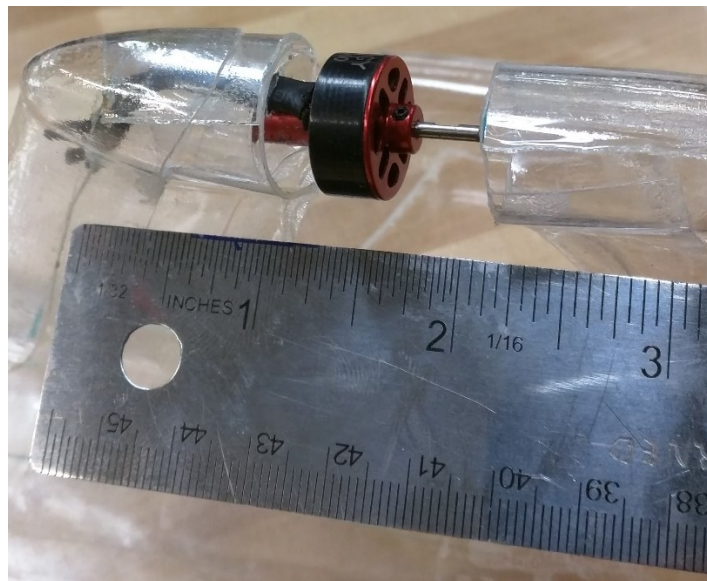


Figure 6.13 Motor mount being secured and glued to the inside of the pod

The same type of polycarbonate glue [30] was used throughout.

This was repeated for all the half airframes which were then ready to be load tested. The next subsection discusses the entire setup of the test.

6.2.2.3 Graphite – Epoxy Airframe

The Half Graphite – Epoxy airframe was available to the author and just needed to be worked on a little to make it load test worthy. First, the flashing was cut and discarded and a Sanding drum attached to a rotary tool was used to achieve smooth edges all around the wings.



Figure 6.14 Smoothing leading edge of lower wing using a sanding drum

The following figures shows the half airframe with the wing spars integrated into the lower wing.



Figure 6.15 Half Graphite – Epoxy airframe

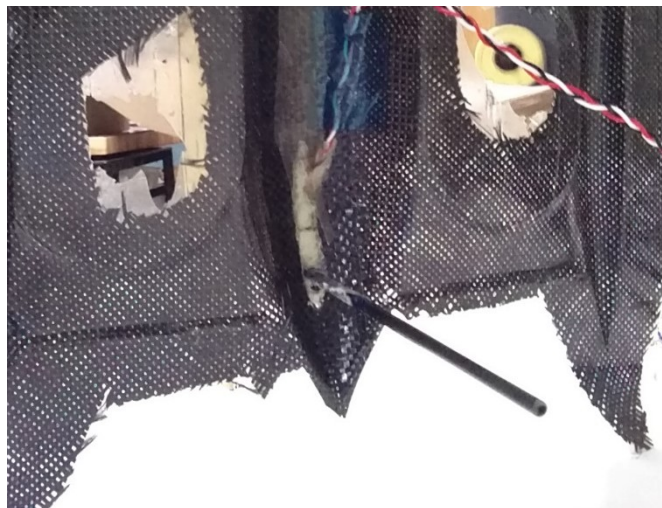


Figure 6.16 Wing spar integrated into the lower wing

Polyurethane Foam was used to fill the wings by injecting it before adding the spars. Curing generally takes about 15 – 20 minutes.

6.2.3 Setup

As mentioned in the previous sub-sections the author was only using half airframes of the XQ-139A to perform the load tests. This meant that only one wing would be tested under a range of point loads applied to its wing tip (pod). The wings would be oriented horizontally relative to the ground and vertical loads would be applied. The vertical deflection of the wing would be measured, in millimeters, for every time a load is applied. The author had to figure out a way where the fuselage and the ‘open’ wings on the side were securely fastened so that they would not interfere with the deflection of the wing undergoing the loads. This was achieved by fixing the airframe down to 2 octant molds of the airframe, placed back-to-back as shown in the figure below.

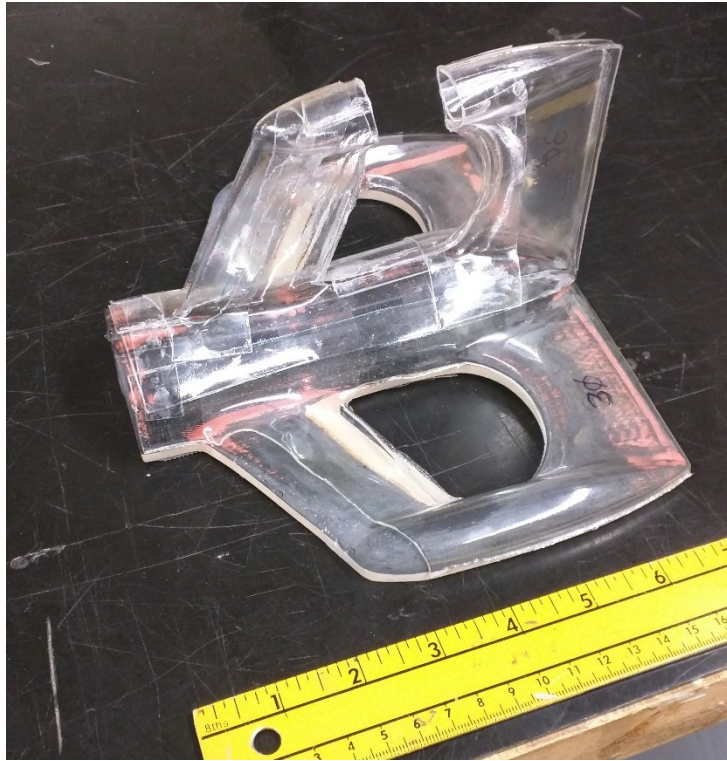


Figure 6.17 Half airframe sitting on the 2 octant molds for support

This allowed ample support to both, the entire fuselage section as well as the open wings. All the author wanted now was to securely fix this setup vertically to carry on with the load tests. A thick rectangular board of MDF (Medium Density Fiberboard) was used as a back support that would be fastened to a table vice.

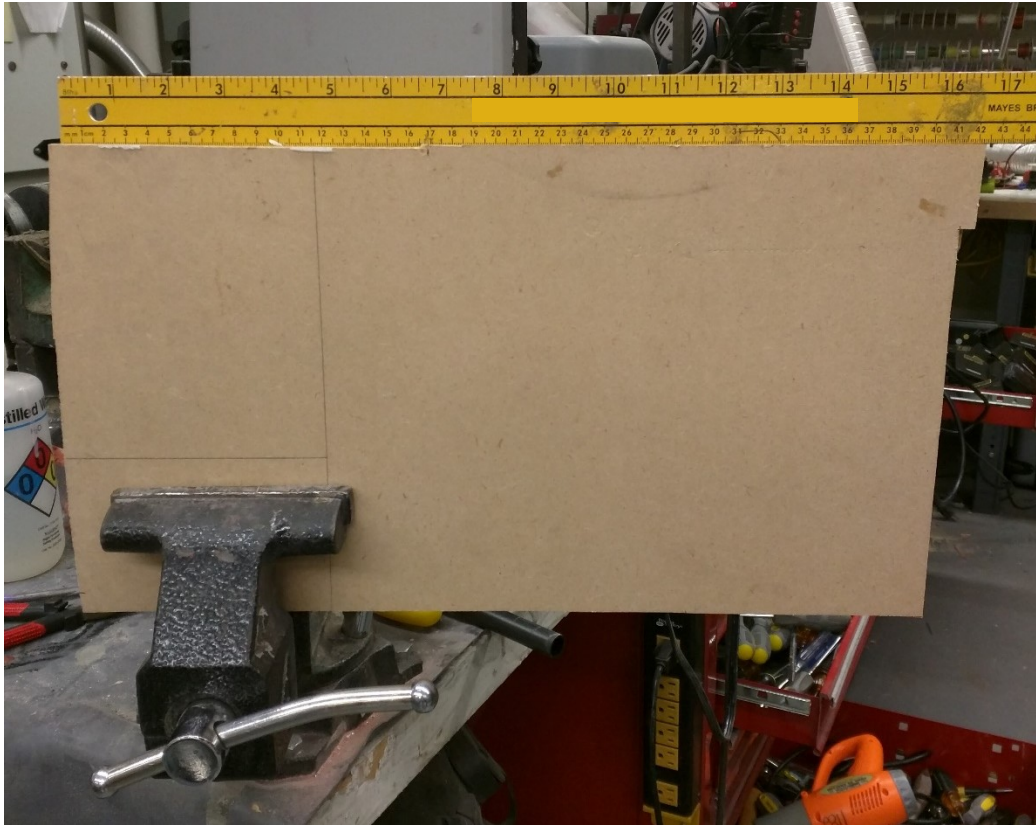


Figure 6.18 MDF (Medium Density Fiberboard) being fastened by the table vice

The 2 octant molds along with the half airframe to be tested were placed on the MDF board and clamped down on four locations to secure the molds to the board, as well as the airframe to the molds.



Figure 6.19 Half airframe and octant molds fastened to the MDF

The author planned to use pre-calibrated weights to apply loads to the wing tips. They were marked in Grams and ranged from 10g – 1000g.

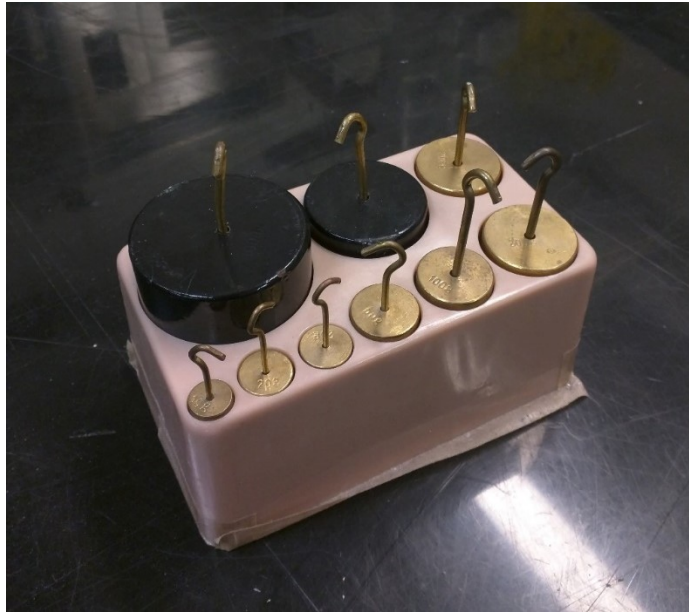


Figure 6.20 Pre-calibrated weights used for load testing

The simplest way to use these weights was to hang them from a strong thread that would wrap around the region the author wanted the load to be applied from. To achieve that, there needed to be a secure point on the pod to hang this thread from.

The author developed a load carrying cap that would be placed over the entire wing tip section around which the thread would be wrapped and tied. This cap was simply a section of the pod and part of the wings that was fabricated by vacuum forming regular airframe octants. The desired sections were cut out and used.



Figure 6.21 Load carrying cap

These load carrying caps were placed and fastened over the half airframe pod and wings by taping it down. After the thread was tied around this cap, the loads were ready to be added.



Figure 6.22 Thread tied around load carrying cap

The only thing left now was to fix a scale alongside the pod to measure the wing deflection when the loads were added. To maintain high accuracy, a thin carbon rod was fastened to the pod as shown in the figure below to point to the scale.

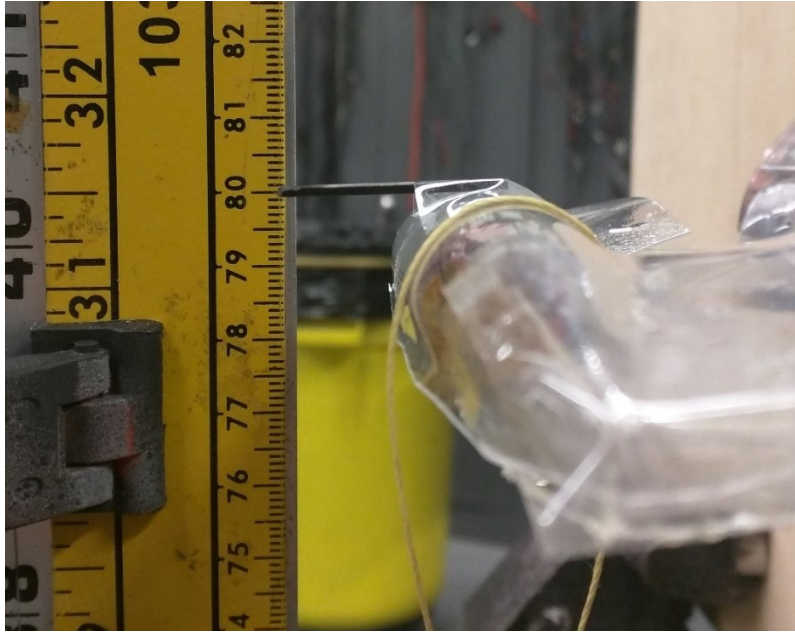


Figure 6.23 Thin carbon rod taped to wing tip

This would indicate the exact reading on the scale for the author to note down during the load tests.

To securely fasten the scale, another vice was used and kept on the floor.



Figure 6.24 Scale clamped to vice on the floor

The setup was complete and ready to go.

6.2.4 Results

After the setup of the test was complete, the author began the Load tests. The procedure for every test was to add weights in increments and note down the corresponding deflections of the wing tip. This was done until either one of the wing fails or deflection reaches 80 mm, although deflection of just 12 mm would cause the propellers to touch.

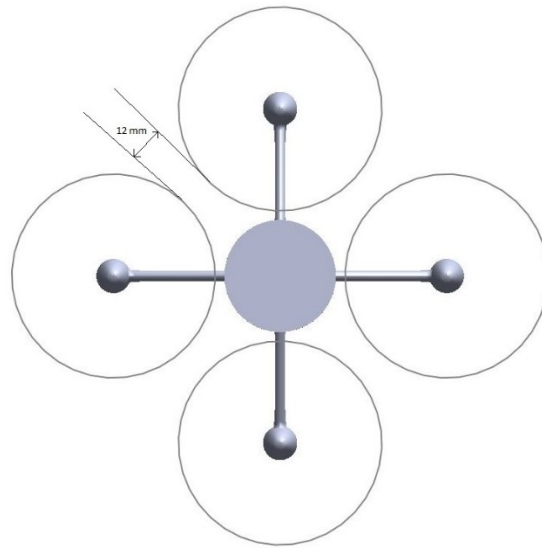


Figure 6.25 Top View of XQ-139 A CAD showing 12 mm clearance between propellers (Scale 1:4)

The following subsections show the figures of each type of polycarbonate airframe, at crucial stages, that the author tested. The entire data of these tests are then compiled in a table that represent the deflection of each type against the corresponding load applied to it. The deflection of the Graphite – Epoxy airframe wings are also included in the test results. Following that is the plot that illustrates the trend of the wing deflection with change in load for the airframes of different thicknesses, with and without spars present. This plot also includes the deflection of the original XQ-139A airframe with and without spars present in its wing.

6.2.4.1 XQ-139A Half Airframe of thickness, 10 mil

The figure below shows the trailing edge of the lower wing getting buckled at load of 311 lbs-f that has caused the joint to fail.

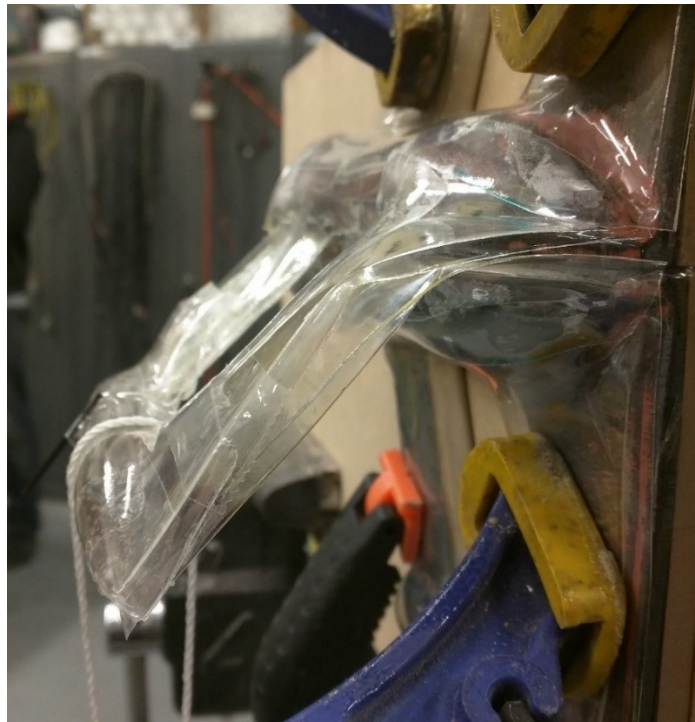


Figure 6.26 Buckling at the trailing edge of the lower wing of the monocoque 10 mil thick airframe wing

The figures below show the wings under 445 lbs-f of vertical load, where the vertical deflection was 82 mm. There is extreme buckling near the lower wing root. There was no sign of structural failure in spite the amount of buckling involved.



Figure 6.27 Extreme buckling near the lower wing root of the monocoque 10 mil thick airframe

6.2.4.2 XQ-139A Half Airframe of thickness, 15 mil

The figure below shows slight buckling occurring on the lower wing at a load of 534 lbs-f.



Figure 6.28 Buckling at the trailing edge of the lower wing of the monocoque 15 mil thick airframe wing

The figure below shows extreme buckling similar to the one occurring on the 10 mil thick monocoque airframe. At this point the wing was under a load of 667 lbs-f.

Once more, there was no structural failure at the wing or fuselage.



Figure 6.29 Extreme buckling near the lower wing root of the monocoque 15 mil thick airframe

6.2.4.3 XQ-139A Half Airframe of thickness, 20 mil

There was buckling at the trailing edge of the lower wing, very similar to the one in the 10 mil thick monocoque airframe, occurring at a load of 1112 lbs-f. There were 2 locations on the trailing edge where the buckling occurred. This is shown in the figure below.



Figure 6.30 Buckling at the trailing edge of the lower wing of the monocoque 20 mil thick airframe wing

There was extreme buckling at a load of 1334 lbs-f near the lower wing root and is shown in the figure below.



Figure 6.31 Extreme buckling near the lower wing root of the monocoque 20 mil thick airframe

6.2.4.4 XQ-139A Half Airframe of thickness, 30 mil

The author was out of the pre-calibrated weights after applying a load of 1334 lbs-f, which is why dumbbells weighing 5 and 10 lbs were added to 890 lbs-f and 445 lbs-f weights to obtain total weights of 1900 lbs-f and 2463 lbs-f respectively. Steel wires were used to hang these dumbbells off the pre-calibrated weights, as shown in the figure below.



Figure 6.32 5 lbs dumbbell hung using a steel wire

At the load of 1900 lbs-f buckling occurred at the trailing edge of the lower wing as shown in the figure below.



Figure 6.33 Buckling at the trailing edge of the lower wing of the monocoque 30 mil thick airframe wing

While the load of 2463 lbs-f was applied, there was a deflection of 81 mm but the load bearing cap failed, as the thread tore through it. The failure of this cap is not considered an airframe failure.

This failure is shown in the figures below.

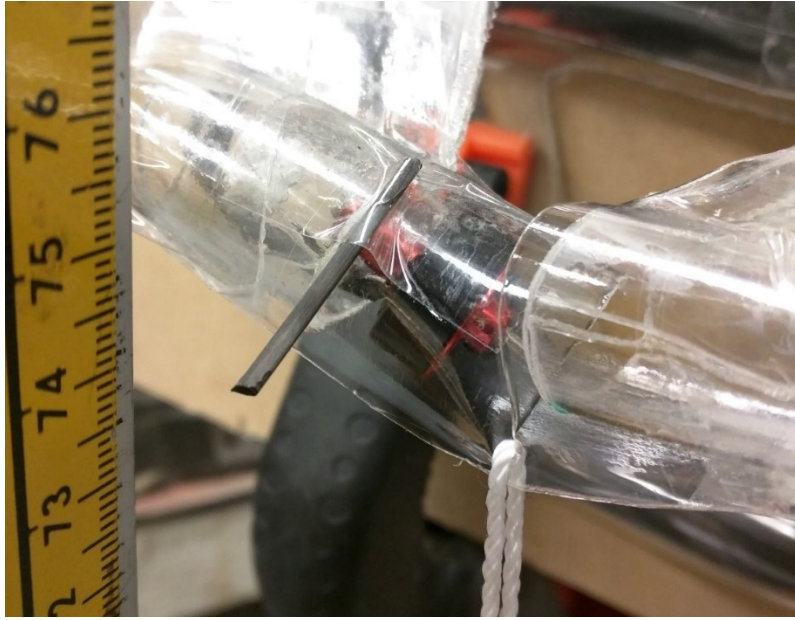


Figure 6.34 Failure of the load carrying cap undergoing a load of 2463 lbs-f



Figure 6.35 Failed load carrying cap

6.2.4.5 XQ-139A Half Airframe of thickness, 10 mil with spars

The author noticed that there was a failure of the lower wing cap at a load of 445 lbs-f. This failure is shown in the figure below.



Figure 6.36 Failure occurring at the lower wing cap of the 10 mil thick half airframe with spars

The figure below suggests that failure occurred because there was no noticeable buckling of the lower wing because of the presence of the spar and hence the load moved all the way to the root of the wing.



Figure 6.37 Almost no buckling along the trailing edge of the lower wing of the 10 mil thick half airframe with spars

6.2.4.6 XQ-139A Half Airframe of thickness, 15 mil with spars

There was absolute failure of the lower wing due to excessive buckling at a load of 756 lbs-f. The deflection of the wing at that point was 85 mm. The figures below show the extent to which the trailing edge had buckled.



Figure 6.38 Significant buckling causing failure at the trailing edge of the lower of the 15 mil thick half airframe with spars



Figure 6.39 Extreme buckling at trailing edge of the 15 mil thick half airframe with spars causing it to open up

6.2.4.7 XQ-139A Half Airframe of thickness, 20 mil with spars

The figure below shows a very noticeable failure occurring at the trailing edge of the lower wing at a load of 756 lbs-f. The deflection of the wing tip was 61 mm at that point.



Figure 6.40 Failure at the trailing edge of the lower wing of the 20 mil thick half airframe with spars

6.2.4.8 XQ-139A Half Airframe of thickness, 30 mil with spars

Failure occurred at the fuselage section where 2 quadrants were glued together at the rear of the airframe. The deflection at this point was 88 mm at a load of 2463 lbs-f.

This failure is shown in the figure below.



Figure 6.41 Failure occurring due to the fuselage section overlap opening up in the 30 mil thick half airframe with spars

6.2.4.9 Graphite – Epoxy Half Airframe with spars

There was very little deflection of the wing, mainly due to the presence of the spar in the lower wing. The figure below shows this slight deflection despite being loaded at 1335 lbs-f.



Figure 6.42 Slight deflection of the Graphite – Epoxy airframe at

6.2.4.10 Graphite – Epoxy Half Airframe without spars

The deflection of the wings without the presence of the spar is significant compared to the airframe with one. The figure illustrates the high deflection of the wing.



Figure 6.43 High deflection of the Graphite – Epoxy wing without spars

6.2.4.11 Test Comparison

Table 6.1 Comparison of wing deflections at various loads between different types of airframes

| Weight, lbs-f | Thickness of polycarbonate, mil | Wing tip deflection, mm | | | | | | | | | |
|------------------|---------------------------------------|-------------------------|----|----|----|----------------|---------------|----------------|----------------|----------------------------------|---------------------------------|
| | | 10 | 15 | 20 | 30 | 10 w/ spars | 15w/ spars | 20 w/ spars | 30 w/ spars | Graphite – Epoxy w/o Spars | Graphite – Epoxy w/ Spars |
| 4.4 | | 1 | 0 | 0 | 0 | 1 | 0 | 0 | 0 | 0 | 0 |
| 22 | | 6 | 2 | 1 | 0 | 6 | 4 | 1 | 1 | 1 | 0 |
| 44 | | 11 | 4 | 2 | 1 | 13 | 8 | 4 | 2 | 2 | 1 |
| 89 | | 21 | 8 | 4 | 2 | 22 | 15 | 8 | 4 | 4 | 2 |
| 222 | | 47 | 21 | 14 | 6 | 53 | 29 | 24 | 10 | 10 | 4 |
| 311 | | 62 | 30 | 17 | 10 | 66 | 38 | 33 | 16 | 14 | 6 |
| 445 | | 82 | 48 | 21 | 14 | | 50 | 43 | 24 | 17 | 8 |
| 534 | | | 59 | 25 | 18 | | 59 | 49 | 28 | 21 | 10 |
| 667 | | | 86 | 31 | 25 | | 78 | 57 | 33 | 28 | 12 |
| 756 | | | | 35 | 28 | | 85 | 61 | 36 | 32 | 14 |
| 890 | | | | 43 | 34 | | | | 41 | 39 | 16 |
| 979 | | | | 47 | 39 | | | | 48 | 45 | 18 |
| 1112 | | | | 67 | 39 | | | | 53 | 62 | 20 |
| 1201 | | | | 72 | 41 | | | | 55 | 66 | 21 |
| 1335 | | | | 79 | 45 | | | | 59 | 72 | 25 |
| 1899 | | | | | 60 | | | | 69 | | |
| 2463 | | | | | 81 | | | | 88 | | |

The table shown above is the amalgamation of all the wing tip deflection of all the types of airframes the author has tested, with corresponding load increments.

By plotting these results of wing deflection against loads applied, the author obtained the figure below to compare all the types of airframes.

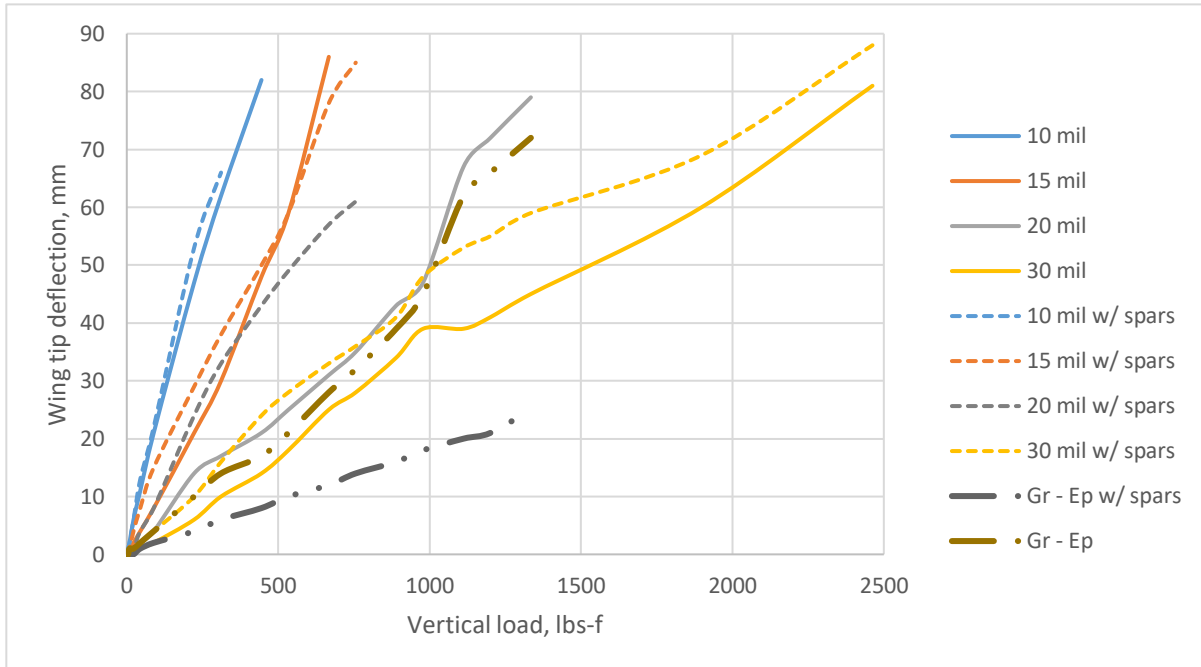


Figure 6.44 Comparison of deflection plots of all types of XQ-139A airframes

By observing the result, the author noticed that the deflection trends of the polycarbonate wings with the spars were not too different to the ones without them. The only exception was the 20 mil thick airframe with the spars. The author suspects that this was solely due to the failure at its wing tip that caused the deflection slope to be almost as much as that of the 15 mil thick airframes. At that point of failure the test for the 20 mil thick airframe with the spars was concluded.

Based on the results, the author believes that the way the spars were integrated into the polycarbonate wings provided no additional structural advantage to resist bending. This could have

been because the spars did not extend beyond the wing root and in fact, would have added unnecessary weight to aid the deflection unlike the original XQ-139A. [31]

In the Graphite – Epoxy airframe with the spar present, there was very little deflection compared to the one without it. The author, therefore, believes that having a spar spanning from tip – to – tip along the entire airframe is much more structurally advantageous.

Although the author has taken the wings into extreme deflection under unrealistic loading conditions, the primary objective as seen earlier in this chapter, was to assess the loads at which failure occurred, if any. The author also wanted to check the load at which the wing undergoing the load would deflect just enough for the propeller to touch one of its neighboring propellers.

The author considered a load equivalent to the total weight of the aircraft as the most extreme condition a single set of wings would go through during actual flight. If the wings have resisted the deflection so that there is no propeller contact, at that load, without failing, the author believes that that is when the airframe would pass the load test.

The table below shows the different types of airframes and the approximate total weight the whole aircraft would be.

Table 6.2 Total Weight comparison of different types of XQ-139A airframes

| Type of XQ-139A airframe | Weight of airframe, g | Weight of electronics and propellers, g | Estimated total weight, g | Equivalent load, lbs-f |
|----------------------------------|-----------------------|---|---------------------------|------------------------|
| 10 mil thick monocoque airframe | 33 | 118 | 151 | 67 |
| 15 mil thick monocoque airframe | 44 | 118 | 162 | 72 |
| 20 mil thick monocoque airframe | 62 | 118 | 180 | 80 |
| 30 mil thick monocoque airframe | 95 | 118 | 213 | 95 |
| 10 mil thick airframe with spars | 37 | 118 | 155 | 69 |
| 15 mil thick airframe with spars | 48 | 118 | 166 | 74 |
| 20 mil thick airframe with spars | 66 | 118 | 184 | 82 |
| 30 mil thick airframe with spars | 99 | 118 | 217 | 97 |

The section of 'Weight of the Electronics and Propellers' in the table, include the following: [31]

- Motor: 9.3g x 4
- Propeller: 1.3g x 4
- 6A ESC: 4.1g x 4
- Control Board: 18.4g x 1
- Power cable: 1.7g x 1
- Receiver: 8.7g x 1
- Battery: 30g x 1

Since the wings can only deflect 12 mm in any direction without allowing the propellers to touch, the author developed a table that shows which airframes would have propeller contact when the extreme load is applied to one set of wings. Once again, the extreme load considered would be the total aircraft weight being applied on the wings.

Table 6.3 Airframes undergoing propeller contact at extreme flight loads

| Type of XQ-139A airframe | Estimated total load applied on one set of wings, g | Wing deflection limit, mm | Wing deflection, mm |
|----------------------------------|---|---------------------------|---------------------|
| 10 mil thick monocoque airframe | 67 | 12 | 16 |
| 15 mil thick monocoque airframe | 72 | 12 | 7 |
| 20 mil thick monocoque airframe | 80 | 12 | 3 |
| 30 mil thick monocoque airframe | 95 | 12 | 2 |
| 10 mil thick airframe with spars | 69 | 12 | 18 |
| 15 mil thick airframe with spars | 74 | 12 | 13 |
| 20 mil thick airframe with spars | 82 | 12 | 7 |
| 30 mil thick airframe with spars | 97 | 12 | 4 |

The airframes undergoing propeller contact would be marked red, since that would be considered as airframe failure. The rest would be marked green.

This data was obtained from the plot shown in Figure 6.44 Comparison of deflection plots of all types of XQ-139A airframes.

The plot has been magnified by the author to make it easier for the reader to see the slight deflection of the wings against the loads.

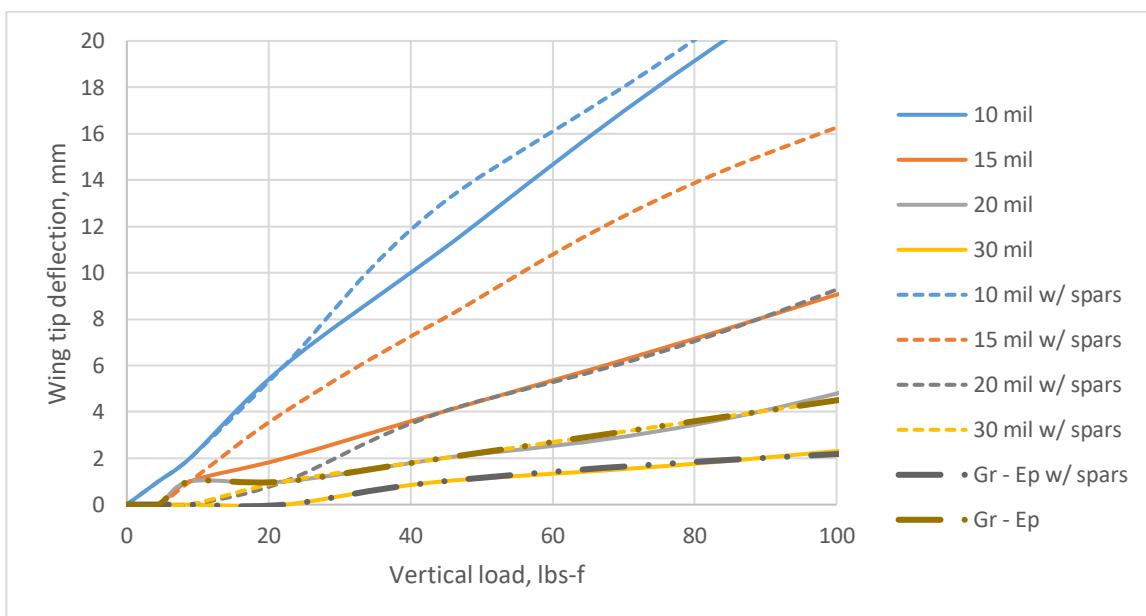


Figure 6.45 Magnified comparison of deflection plots of all types of XQ-139A airframes

From the data provided above, the author confirms that the following airframe types have passed the load tests and the most suitable one must be selected as the final XQ-139A Polycarbonate UAV.

- 15 mil thick monocoque airframe
- 20 mil thick monocoque airframe

- 30 mil thick monocoque airframe
- 20 mil thick airframe with wing spars
- 30 mil thick airframe with wing spars

For any type of aircraft, the higher the Power-to-Weight ratio, the higher the performance.

Hence, it makes sense to use the 15 mil thick monocoque airframe as the default XQ-139A Polycarbonate UAV. This is because it would be the lightest airframe that would meet all the structural demands of the XQ-139A.

Being slightly thicker than the 10 mil, the 15 mil thick polycarbonate would also be easier to use to manufacture the XQ-139A and provide a better quality product. This is because being thicker, it can retain the heat from the vacuum forming process better and be shaped more efficiently.

For the reference of the reader, the author would like to compare the results of the wing load tests with a benchmark. A hollow elliptical beam of polycarbonate has been chosen which has an equivalent chord of 1.5 inches and span of 2.5 inches. It has a maximum thickness in the center of 0.225 inches. Using the dimensions mentioned above, the author performed a few calculations and simulated a cantilever beam deflection test with a point load on its tip, just like the wings of the XQ-139A. The results were plotted against the test results of the polycarbonate airframe. The author calculated the deflection of 4 types of beams of thicknesses, 10, 15, 20 and 30 mil to maintain homogeneity. The results are shown in the plot below.

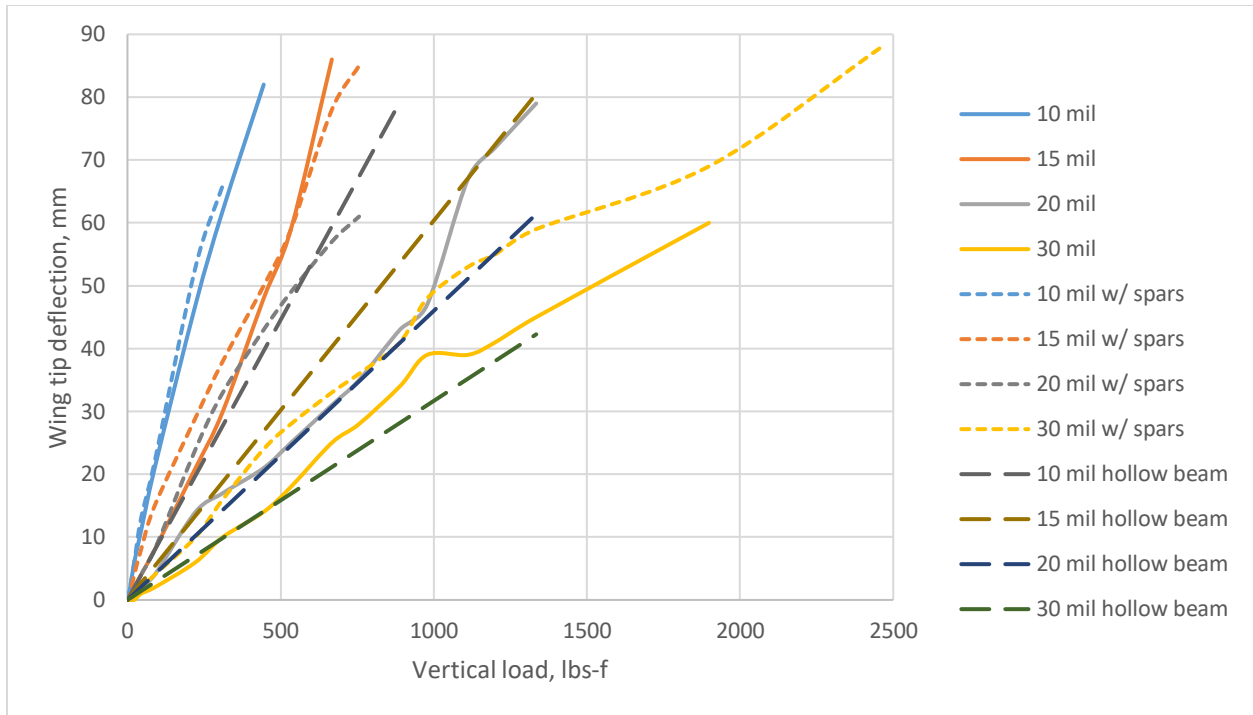


Figure 6.46 Comparing load test results with benchmark tests

As seen in the plot, the wing deflections of the XQ-139A polycarbonate airframes have an overall lower flexural strength compared to the single hollow polycarbonate beam. The only wing types not matching the computational data is the 10 mil and 15 mil thick airframes. After that the trend of the deflection curve almost matches the benchmark tests.

The author believes that integrating complete spars, like in the Graphite – Epoxy airframe would provide much better flexural strength.

6.3 Conclusion and Recommendations

6.3.1 Conclusion

The author concludes that,

- 5 types of Polycarbonate Airframes, listed below passed the load tests:
 1. 15 mil thick monocoque airframe
 2. 20 mil thick monocoque airframe
 3. 30 mil thick monocoque airframe
 4. 20 mil thick airframe with wing spars
 5. 30 mil thick airframe with wing spars
- The 15 mil thick monocoque XQ-139A was chosen as the default Polycarbonate airframe.

6.3.2 Recommendations

The author recommends that,

- Load tests be performed on the Polycarbonate airframes with the wing spars spanning from tip – to – tip, like the spars in the Graphite – Epoxy airframe.
- The load tests be performed by the Instron 3300 Single Column Universal Testing System [32] as it would be a very useful and accurate tool for the deflection tests of the Polycarbonate XQ-139A airframes.

7 Conclusion and Recommendations

7.1 Conclusion

The author would like to conclude that:

- Polycarbonate will be used as the material to manufacture the XQ-139A;
- The vacuum forming process has been chosen for all the polycarbonate molding in this report.
- The 3 stages of Mold Manufacturing were,
 1. Additive Processing – 3D Printing;
 2. Reverse Mold Processing;
 3. Mold Processing;
- The different Mold Components that were manufactured were,
 1. Half Quadrants (Octants) of the XQ-139A Airframe;
 2. Leading edge wing sections (wing caps) of the upper and lower wings.
- A Hot-Wire cutter was designed and assembled for all Polycarbonate cutting processes;
- It took 4 manufacturing iterations to obtain the XQ-139A Polycarbonate Airframe.
- The total material costs for the 2 types of XQ-139A Airframes are;
 1. Carbon Fiber: US \$105
 2. Polycarbonate: US \$23
- The total labor costs for the 2 types of XQ-139A Airframes are;
 1. Carbon Fiber: US \$720
 2. Polycarbonate: US \$60

- The total costs for the 2 types of XQ-139A Airframes are;
 1. Carbon Fiber: US \$825
 2. Polycarbonate: US \$83
- The overall percentage drop in manufacturing costs of the XQ-139A is 89.9%.
- 5 types of Polycarbonate Airframes, listed below passed the load tests:
 1. 15 mil thick monocoque airframe
 2. 20 mil thick monocoque airframe
 3. 30 mil thick monocoque airframe
 4. 20 mil thick airframe with wing spars
 5. 30 mil thick airframe with wing spars
- The 15 mil thick monocoque XQ-139A was chosen as the default Polycarbonate airframe.

7.2 Recommendations

The author recommends that,

- A greater number of molding techniques be discussed to confirm that Vacuum Forming is still the most pragmatic molding process to be used in this report.
- Fast curing Plastic Resin be used against the Slow curing version, to save on processing time by up to 88%.
- A bigger Vacuum former platform be used for the 4 sets of wing caps, to allow more room between each set, to achieve a tighter vacuum mold;
- A second airframe should be manufactured to improve its quality and surface finish.
- A detailed cost analysis be performed for the Polycarbonate XQ-139A.

- Load tests be performed on the Polycarbonate airframes with the wing spars spanning from tip – to – tip, like the spars in the Graphite – Epoxy airframe.
- The load tests be performed by the Instron 3300 Single Column Universal Testing System [32] as it would be a very useful and accurate tool for the deflection tests of the Polycarbonate XQ-139A airframes.
- In order to get a better-quality product of the Polycarbonate airframe, ‘Pressure Vacuum Molding’ be used.

8 Future Work

Due to the restriction of time, the author was unable to achieve something that was not included in the thesis report. Assembling the Polycarbonate 15 mil thick, monocoque XQ-139A with all the required electronic equipment to make it flight worthy and perform flight tests. A successful flight test would validate the load test results and confirm that they were accurate enough to help the author choose the right airframe for the Polycarbonate version of the XQ-139A.

The flight test results can then also be compared to the tests of the Carbon Fiber XQ-139A to see how it compares in performance and other flight characteristics.

9 References

- [1] Anonymous, "Phantom," published by DJI, 2016. [Online]. Available: <http://www.dji.com/phantom>.
- [2] Anonymous, "Predator C Avenger RPA," published by General Atomics, 2016. [Online]. Available: <http://www.ga-asi.com/predator-c-avenger>.
- [3] Smith, E., "game of Drones," February 2015. [Online]. Available: <http://eosmith.com/game-drones/>.
- [4] Anonymous, "MQ-9 Reaper," published by U.S. Air Force, 23 September 2015. [Online]. Available: <http://www.af.mil/AboutUs/FactSheets/Display/tabid/224/Article/104470/mq-9-reaper.aspx>.
- [5] Anderson, S., "Historical Overview of V/STOL Aircraft Technology," *NASA Technical Memorandum 81280*, 1997.
- [6] Anonymous, "HISTORY OF QUADCOPTERS AND OTHER MULTIROTORS," published by Krossblade Aerospace Systems LLC, 2016. [Online]. Available: <http://www.krossblade.com/history-of-quadcopters-and-multirotors/>.
- [7] Pounds, P., Mahony, R. and Corke, P., "Modelling and Control of a Quad-Rotor Robot," in *Australasian Conference on Robotics and Automation*, Auckland, 2006.
- [8] Anonymous, "V-22 Osprey," published by Boeing 2016. [Online]. Available: <http://www.boeing.com/defense/v-22-osprey/>.
- [9] Anonymous, "X-22A Tri-Service V/STOL Aircraft," published by Bell Aerospace Company, Buffalo, 1969.
- [10] Anonymous, "AW609," Published by Leonardo – Finmeccanica, 2016. [Online]. Available: http://www.leonardocompany.com/en/product-services/elicotteri_helicopters/aw609.
- [11] Anonymous, "THE X-19 V/STOL TECHNOLOGY - A CRITICAL REVIEW," published by Curtiss-Wright, Air Force Flight Dynamics Laboratory, Wood-Ridge,, 1967.
- [12] Bramlette, R.B., and Barrett, R. M., "Design and Flight Testing of a Convertible Quadcopter for Maximum Flight Speed," Lawrence, Expected 2017.

- [13] Anonymous, "Vacuum Forming," published by British Plastics Federation, 2016. [Online]. Available: http://www.bpf.co.uk/plastipedia/processes/vacuum_forming.aspx.
- [14] Anonymous, "Vacuum Forming," published by Shelley Thermoformers Int'l, 2016. [Online]. Available: <http://www.cannonshelley.com/en/D-Thermof.-Applications/vacuum-forming.html#>.
- [15] Anonymous, "Polycarbonates (PC)," published by Granule Group, 2016. [Online]. Available: [http://www.granulegroup.com/en/products/181/Polycarbonates-\(PC\)](http://www.granulegroup.com/en/products/181/Polycarbonates-(PC)).
- [16] Cornejo, A., "Injection Moulding," 2015. [Online]. Available: https://en.wikipedia.org/wiki/Injection_moulding#/media/File:Injection_molding_diagram.svg.
- [17] Beall, G., "Rotational Molding," 1998.
- [18] Anonymous, "Rotational Moulding," published by Pentas Moulding BV, 2016. [Online]. Available: <http://www.pentasmoulding.com/production/rotational-molding/>.
- [19] Anonymous, "MAKERBOT REPLICATOR Z18," published by MakerBot, 2016. [Online]. Available: <https://www.makerbot.com/replicator-z18/>.
- [20] Anonymous, "MakerBot MP05950 Replicator Z18 3D Printer," published by Mono Machines, 2016. [Online]. Available: <http://www.monomachines.com/shop/makerbot-replicator-z18-3d-printer.html>.
- [21] Anonymous, "Bondo Glazing & Spot Putty, 4.5 oz," published by Advance Auto Parts, [Online]. Available: http://shop.advanceautoparts.com/p/bondo-glazing-spot-putty-4.5-oz-907/7100876-p?iv=__iv_p_1_a_214327102_g_12425515822_w_pla-61865531738_h_9023850_ii_d_c_v_n_g_x_pla_y_6201684_f_online_o_7100876-P_z_US_i_en_j_61865531738_s_vi_&utm_source=ACQ&utm_medi.
- [22] Anonymous, "Mold Making," published by AEROMARINE PRODUCTS, INC., 2016. [Online]. Available: <https://www.aeromarineproducts.com/product-category/mold-making/>.
- [23] Anonymous, "Smooth-Cast® ONYX® Series," published by Reynolds Advanced Materials, 2016. [Online]. Available: <http://www.reynoldsam.com/product/smooth-cast-onyx/>.
- [24] Anonymous, "Hobby Hot Wire EPS Foam Cutter Table," published by Demand Products, Inc., 2016. [Online]. Available: <http://www.demandproducts.com/Hobby-and-Craft-items/item.php?l1=10,7&sku=HCM2S>.

- [25] Anonymous, "Online catalog," published by TSLOTS, 2016. [Online]. Available: <http://www.tslots.com/onlinecatalog/>.
- [26] Anonymous, "Ryobi 1.2 Amp 16 in. Corded Scroll Saw," published by Home Depot, 2016. [Online]. Available: https://www.google.com/shopping/product/9705940270144247566?lsf=seller:8740,store:9749140554878902463&prds=oid:1599638386180095629&q=scroll+saw&hl=en&ei=rGQ8WLTOEsW_jwTYI5zwCg&mid=syrjdv4k%7Cdc_mtid_8903tb925190_pcrd_50645156379_pkw_pmt_product_205419.
- [27] Bramlette, R., *Cost Estimation of the XQ-139*, 2016.
- [28] Anonymous, "LOCTITE® EPOXY HEAVY DUTY," published by Henkel Corp., 2016. [Online]. Available: http://www.loctiteproducts.com/p/13/23/epxy_heavy/overview/Loctite-Epoxy-Heavy-Duty.htm.
- [29] Anonymous, "Turnigy 1811 brushless Outrunner 2900kv," published by Hobby King, 2016. [Online]. Available: https://hobbyking.com/en_us/turnigy-1811-brushless-outrunner-2900kv.html.
- [30] Anonymous, "IPS Weld-On #4SC Plastic Solvent Glue Cement for Acrylic and Plexiglass," published by Plastic-Craft Products, 2016. [Online]. Available: <https://www.plastic-craft.com/products/weldon4sc>.
- [31] Bramlete, R., *XQ-139 Research Notebook*, 2016.
- [32] Anonymous, "3300 Single Column Universal Testing Systems," published by Illinois Tool Works Inc., 2016. [Online]. Available: <http://www.instron.us/en-us/products/testing-systems/universal-testing-systems/electromechanical/3300/3340-single-column>.

APPENDIX A – Process of Manufacturing the Polycarbonate XQ-139A

Procedure of Manufacturing the Polycarbonate XQ-139A Airframe

Step 1: Fasten 15 mil Polycarbonate sheet on Vacuum Former frame using regular tape, lock the frame to its highest position and turn heating coil on.

Step 2: Arrange 4 Octant mold back to back on vacuum platform till sheet heats up.

Step 3: Once the polycarbonate sheet sags about 2 inches, turn on vacuum switch and force down the frame as fast as possible and hold position for a few seconds before turning off vacuum. Turn heat off.

Step 4: Remove formed sheet from vacuum frame and take molds out. Fasten new sheet on the frame and repeat Steps 1 – 3.

Step 5: Repeat Step 1 and arrange 4 sets of wing cap molds instead of octants.

Step 6: Repeat Step 3 and remove formed sheet from vacuum frame and ensure that vacuum and heat switches are turned off.

Step 7: Remove molds from formed sheet

Step 8: Pass both the formed sheets with the octants through the Hot wire cutter to get rid of the flashing.

Step 9: Cut flashing out of the wing caps sheet.

Step 10: Cut the two sheets to obtain 8 octant polycarbonate sections.

Step 11: Cut out extra flashing to accommodate a sufficient overlap of 2 octant sections to form a quadrant airframe.

Step 12: Use quadrant guide tool to aid in gluing the octants together.

Step 13: Repeat Step 11 & 12 for all octants to obtain a total of 4 quadrant sections.

Step 14: Cut out half an inch of the leading edges of the upper wing, on all quadrants.

Step 15: To stick 2 quadrants together, securely glue pod edge, making sure all other edges are aligned.

Step 16: Glue the trailing edge of the upper wing.

Step 17: Place upper wing cap over the leading edge of the upper wing, all the way down and glue all its edges and press for a few seconds, until dry.

Step 18: Align and place lower wing cap over leading edge of lower wing, apply glue on all its edges and hold in place for a few seconds, until dry.

Step 19: Cut out a 2 inch x 0.5 inch polycarbonate strip of thickness 20 mil and glue on the inside of the open fuselage section between the 2 quadrants.

Step 20: Repeat Steps 15 - 19 for other quadrants to obtain a half airframe.

Step 21: Repeat the same procedure of joining the edges of 2 half airframes, as mentioned in Steps 15 – 19, to obtain full airframe.